BIOCHEMISTRY

Identification and characterization of circulating immune complexes in IgA nephropathy

Yasuyuki Matsumoto[1]†, Rajindra P. Aryal[1]*†, Jamie Heimburg-Molinaro[1], Simon S. Park[2,3], Walter J. Wever[2,3]‡, Sylvain Lehoux[1], Kathrin Stavenhagen[1], Joanna A. E. van Wijk[4], Irma Van Die[5], Arlene B. Chapman[6], Elliot L. Chaikof[2,3], Richard D. Cummings[1]*

The underlying pathology of immunoglobulin A (IgA) nephropathy (IgAN), the most common glomerulonephritis worldwide, is driven by the deposition of immune complexes containing galactose-deficient IgA1 [Tn(+)IgA1] in the glomerular mesangium. Here, we report that novel anti-Tn circulating immune complexes (anti-Tn CICs) contain predominantly IgM, representing large macromolecular complexes of ~1.2 megadaltons to several megadalton sizes together with Tn(+)IgA1 and some IgG. These complexes are significantly elevated in sera of patients with IgAN, which contains higher levels of complement C3, compared to healthy individuals. Anti-Tn CICs are bioactive and induce specific proliferation of human renal mesangial cells. We found that these anti-Tn CICs can be dissociated with small glycomimetic compounds, which mimic the Tn antigen of Tn(+)IgA1, releasing IgA1 from anti-Tn CICs. This glycomimetic compound can also significantly inhibit the proliferative activity of anti-Tn CICs of patients with IgAN. These findings could enhance both the diagnosis of IgAN and its treatment, as specific drug treatments are now unavailable.

INTRODUCTION

Immunoglobulin A (IgA) nephropathy (IgAN), also known as Berger's disease (*1*), is the most predominant form of primary glomerulonephritis worldwide, accounting for ~30% of the terminal renal failures in patients within 10 to 20 years after diagnosis (*2*–*7*). The pathogenesis of IgAN is driven by the mesangial granular deposition of immune complexes (ICs) containing IgA1 (*8*, *9*). IgAN demonstrates significant clinical variability arising from the underlying genetic and environmental complexity contributing to the disease pathology. The cause of the majority of primary IgAN cases worldwide is unknown, as the condition is largely sporadic, and only a minority of cases have been reported within clusters of families (*10*).

A contributing component to IgAN is the unusual nature of the glycosylation of IgA1. Unlike IgA2, IgA1 contains 22 amino acids in a hinge region (HR), composed primarily of Ser/Thr/Pro residues, in which three to six of the nine Ser/Thr residues may be modified by *O*-glycans (*11*, *12*). Examples of these glycans on IgA1 include the Tn antigen GalNAcα1-Ser/Thr [here designated Tn(+)IgA1 and also termed galactose-deficient IgA1], along with monosialyl and/or disialyl core 1 structure Galβ3GalNAcα1-Ser/Thr [here designated Tn(−)IgA1] (*13*, *14*). Any form of Tn antigen on IgA1 is considered Tn(+)IgA1 irrespective of serum from healthy control and patient with IgAN. Total IgA1 is frequently elevated in sera of patients with IgAN (*8*, *9*, *15*–*19*), and some of those studies indicate that there is an accompanying elevation of the Tn(+)IgA1 glycoform. While circulating IgA1 contains mixtures of these two major glycoforms, Tn(+)IgA1 and Tn(−)IgA1, the relative proportion of these two glycoforms does not appear to be statistically different in patients, but the overall elevation of IgA1 in patients leads to a concomitant rise in both glycoforms (*13*, *14*).

Earlier, we observed that individuals infected by certain parasites express IgM antibodies to Tn antigen (*20*, *21*). The Tn antigen is commonly expressed in the glycoconjugates of many insects and pathogens (*22*, *23*). This suggested to us that human exposure to this antigen is perhaps frequent and prompted us to explore the potential role of such antibodies to the Tn antigen within Tn(+)IgA1 and their potential to form ICs with IgA1. Although ICs containing the Tn(+)IgA1 glycoform have been proposed to be associated with the IgAN pathology, little is known about the exact nature of such complexes (*24*). The formation of such complexes is a crucial aspect of the currently existing model of the pathogenesis of IgAN, where a multihit hypothesis involves autoantibody production and altered expression of Tn(+)IgA1 glycoforms (*8*). The emerging picture suggests that the Tn(+)IgA1 glycoform associates with anti–IgA1-specific IgG, IgA, or IgM antibodies to form large macromolecular ICs, depositing in the mesangium and ultimately responsible for disease pathology (*8*, *25*–*29*).

To explore this concept in more detail, we developed an affinity approach to isolating and exploring the nature of the anti-Tn circulating ICs (anti-Tn CICs) associated with Tn(+)IgA1 from human sera. We identified novel anti-Tn CICs of large macromolecular assemblies, predominantly containing IgM together with Tn(+)IgA1 and some level of IgG. We measured the level of such antibodies, where we found a correlation with IgAN diagnosis. Such anti-Tn CICs can be disrupted by glycomimetics, which block recognition of the Tn antigen, releasing IgA1 from such complexes. In addition, the glycomimetic compound blocks the proliferative activity of anti-Tn CICs toward primary human renal mesangial cells (HRMCs). These results have important implications for the diagnosis and potential treatment of IgAN.

[1]Department of Surgery, Beth Israel Deaconess Medical Center, Harvard Medical School, Boston, MA, USA. [2]Department of Surgery, Center for Drug Discovery and Translational Research, Beth Israel Deaconess Medical Center, Harvard Medical School, Boston, MA, USA. [3]Wyss Institute of Biologically Inspired Engineering, Harvard University, Boston, MA, USA. [4]Department of Pediatric Nephrology, Amsterdam University Medical Centre, location VUmc, Amsterdam, Netherlands. [5]Department of Molecular Cell Biology and Immunology, Amsterdam University Medical Centre, Vrije Universiteit Amsterdam, Amsterdam, Netherlands. [6]Department of Medicine, Section of Nephrology, University of Chicago School of Medicine, Chicago, IL, USA.
*Corresponding author. Email: rparyal@bidmc.harvard.edu (R.P.A.); rcummin1@bidmc.harvard.edu (R.D.C.)
†These authors contributed equally to this work.
‡Present address: Ferring Pharmaceuticals, San Diego, CA, USA.

RESULTS

Presence of anti-Tn antibodies that are specific to Tn(+)IgA1 in normal human sera

To gain insight into anti-Tn antibodies in human sera and their impact on IgAN pathogenesis, we prepared a high-density Tn antigen matrix [Tn(+)matrix] composed of Asialo–bovine submaxillary mucin (Asialo-BSM), a mucin containing a high amount of Tn antigen along its backbone of primarily Ser, Thr, and Pro residues and potentially mimicking the HR of IgA1 in many respects (*17*, *30*). We reasoned that this Tn(+)matrix could be used to affinity-purify anti-Tn antibodies from human sera (fig. S1A). As this Tn(+)matrix specifically interacts with a defined anti-Tn antibody and lectin in control studies (fig. S1, B and C), we used this matrix to affinity-purify anti-Tn antibodies that are potentially present in human sera. The bound materials were resolved on SDS–polyacrylamide gel electrophoresis (PAGE) and were Coomassie-stained. We observed three to four major Coomassie-stained bands only in the material that bound to the Tn(+)matrix. The protein sizes ranged between

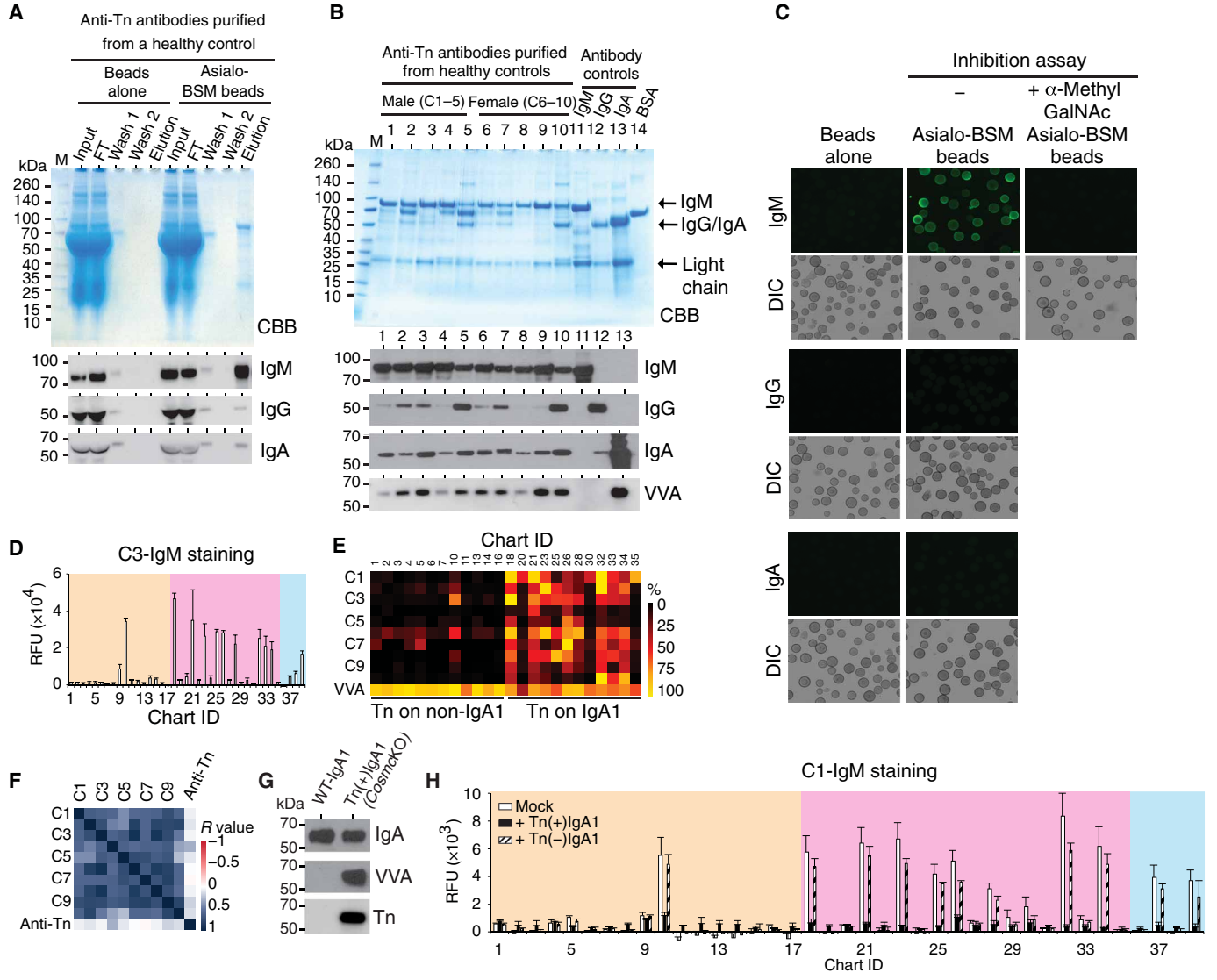

Fig. 1. Anti-Tn antibodies in human sera: Identification and characterization. (**A**) Coomassie-stained SDS-PAGE analysis of affinity-purified anti-Tn antibodies from serum using Tn(+)matrix (elution) and control (beads alone); affinity-purified materials (top) immunoblotted as indicated (bottom). FT, flow through. Coomassie brilliant blue (CBB)-stained. (**B**) Similar analysis to (A) (healthy donors; Table 1), with purified control antibodies and bovine serum albumin (BSA) (4 μg); VVA detects Tn(+)IgA1. (**C**) Purified anti-Tn antibodies bind to Tn(+) matrix; α-methylGalNAc inhibits binding (Alexa Fluor 488–labeled anti-human IgM antibody, top, green). Four times amount of anti-Tn antibodies mixed with Tn(+)matrix [Alexa Fluor 488–labeled anti-human IgG (middle) and IgA (bottom)]. Beads alone, negative control; Differential Interference Contra (DIC), bead images. Performed in three biological replicates (C1, C6, and C10). (**D**) Tn glycopeptide array probed with purified anti-Tn antibodies from 10 healthy control sera (C3, representative) and stained with Alexa Fluor 488–labeled anti-human IgM antibody (see fig. S3). Chart ID corresponds to Table 2. (**E** and **F**) Data analysis using GLAD (Glycan Array Dashboard), comparing binding preferences between Tn on IgA1 and non-IgA1 peptides, and correlation of binding patterns in C1 to C10. VVA binds Tn glycopeptides (positive control), and anti-Tn (recombinant murine anti-Tn IgM) differs from C1 to C10 binding. (**G**) Purified Tn(+)IgA1 (from *Cosmc*KO cells) and Tn(–)IgA1 (WT) analyzed by SDS-PAGE Western blot (WB), probed with purified anti-Tn antibodies (bottom), VVA (middle), and loading control (IgA; top), $n = 3$. (**H**) Tn glycopeptide array probed with purified anti-Tn antibody (C1) after preincubation with purified Tn(+)IgA1 or Tn(–)IgA1 and stained with Alexa Fluor 647–labeled anti-human IgM. For Tn glycopeptide arrays, error bars represent ±1 SD of four replicates. RFU, relative fluorescence units.

~25 and 75 kDa (Fig. 1A, top, elution lane), suggesting heavy chains and light chains of antibodies. The same preparation was immunoblotted with specific antibodies, which demonstrated that the bound material contains IgM, IgA, and IgG (Fig. 1A, bottom). We further characterized the Tn(+)matrix-purified anti-Tn antibodies from the sera of 10 different healthy individuals (Table 1), using appropriate controls as indicated on the top of the Coomassie-stained gel. These results demonstrate that the purified anti-Tn antibodies from each sample are predominantly IgM (75 kDa), along with lesser amounts and varying proportions of IgG (50 kDa) and/or IgA (55 kDa) (Fig. 1B). Immunoblots confirmed that IgM is present in all samples along with varying amounts of IgG; the Tn(+)IgA1 glycoform was also present in all samples (Fig. 1B, bottom). To further confirm that the identified proteins are immunoglobulins (Fig. 1B), we performed proteomic analyses by mass spectrometry (MS) on individual sera samples from five controls (C1, C2, C3, C6, and C7). The results demonstrate that the Coomassie-stained bands represent IgM, IgG, and IgA, as expected (fig. S2 and table S1). The results of proteomic analyses demonstrate that additional proteins are present, including the consistent presence of complement C3.

To investigate whether the interaction of the anti-Tn antibodies to the Tn(+)matrix is Tn antigen dependent, we used fluorescent-tagged secondary antibodies to image the antibodies bound to the Tn(+)matrix. We observed strong staining for bound IgM (Fig. 1C, top, green fluorescent) but no significant staining for either IgG or IgA (Fig. 1C, middle and bottom). Either the IgG and IgA1 levels in the bound material are thus relatively low, or these antigens could be cryptic within complexes and inaccessible in the context of the beads. Nevertheless, using this approach, we asked whether binding of antibodies to Tn(+) matrix can be inhibited by a hapten sugar α-methylGalNAc (a glycomimetic derived from the Tn antigen). Binding of antibodies to the Tn(+)matrix was completely inhibited by α-methylGalNAc pretreatment (Fig. 1C, top right), thus demonstrating that the interaction is Tn antigen dependent. These results demonstrate that healthy individuals contain low levels of anti-Tn antibodies that specifically recognize the Tn antigen in a hapten-inhibitable fashion.

To examine the specificity of antibodies to the Tn antigen, one of the approaches that we took was to prepare a synthetic Tn glycopeptide array, where small glycopeptides contain the Tn antigen in the context of IgA1 HR [Tn(+)IgA1 glycopeptides], or within non-IgA1 peptides as listed (Table 2). We applied the affinity-purified antibodies from sera of 10 healthy individuals and detected for the presence of bound IgM. The results demonstrate higher interaction of such IgM with Tn(+)IgA1 glycopeptides compared to other Tn(+)non-IgA1 glycopeptides (Fig. 1, D to F, and fig. S3A). In parallel experiments, we also probed the preparation of this glycopeptide array for the possible binding of IgA1 and IgG using amounts that were increased fourfold as compared to IgM detection. We did not detect signals above background (fig. S3, B and C). Thus, these results indicate that either IgA1 or IgG does not bind the Tn(+)IgA1 glycopeptides or such antibodies are not available within potential complexes, whereas IgM is available and accessible. In addition, we also tested binding of antibodies to the CFG (Consortium for Functional Glycomics) mammalian glycan microarray—this array contains some glycans expressing terminal GalNAc but lacks any glycopeptides or

Table 1. Basic donor information. M, male; F, female.

Healthy donor			Patient with IgAN		
No.	**Age (years)**	**Sex**	**No.**	**Age (years)**	**Sex**
C1	48	M	P1	37	M
C2	30	M	P2	64	M
C3	28	M	P3	41	M
C4	55	M	P4	49	F
C5	23	M	P5	58	F
C6	24	F	P6	47	F
C7	30	F	P7	50	F
C8	27	F	P8	62	M
C9	58	F	P9	22	M
C10	53	F	P10	54	M
C11	20	M	P11	21	M
C12	15	M	P12	19	F
C13	12	M	P13	18	F
C14	21	M	P14	20	M
C15	15	F	P15	17	M
C16	16	F	P16	15	M
C17	19	M	P17	9	M
C18	23	M	P18	21	M
C19	30	F	P19	11	M
C20	10	F	P20	21	M
	M:F ratio = 11:9			M:F ratio = 14:6	

Table 2. Structures on Tn glycopeptide array. IDs 1 to 17, Tn antigen on non-IgA1; IDs 18 to 35, Tn antigen on IgA1; IDs 36 to 39, control glycans; asterisk (*), GalNAc (Tn) residue on Ser or Thr.

ID	Detail	Sequence
1	A-MUC2	Ac-PT*TTPLK-NH_2
2	B-MUC2	Ac-PTT*TPLK-NH_2
3	C-MUC2	Ac-PTTT*PLK-NH_2
4	D-MUC2	Ac-PT*T*TPLK-NH_2
5	E-MUC2	Ac-PT*TT*PLK-NH_2
6	F-MUC2	Ac-PTT*T*PLK-NH_2
7	G-MUC2	Ac-PT*T*T*PLK-NH_2
8	R-MUC2	Ac-PTTTPLK-NH_2
9	a-Dystroglycan	Ac-PPTTTTKKP-NH_2
10	MUC5AC	H_2N-GTTPSPVPT*TSTTSAP-OH
11	EA2	Ac-PTTDSTT*PAPTTK-NH_2
12	EA2-R	Ac-PTTDSTTPAPTTK-NH_2
13	a-Dystroglycan	Ac-PPT*T*T*T*KKP-HN_2
14	MUC1–1	H_2N-TSAPDT*RDAP-NH_2
15	MUC1–1R	H_2N-TSAPDTRDAP-NH_2
16	MUC1–2	H_2N-APGS*T*APP-NH_2
17	MUC1–2R	H_2N-APGSTAPP-NH_2
18	IgA-Pep01	H_2N-KPVPST*PPT*PS*C-OH
19	IgA-Pep02	H_2N-KPVPSTPPTPSC-OH
20	IgA-Pep03	H_2N-KPVPS*TPPTPSC-OH
21	IgA-Pep04	H_2N-KPST*PPT*PS*PS*C-OH
22	IgA-Pep05	H_2N-KPSTPPTPSPSC-OH
23	IgA-Pep06	H_2N-KT*PPT*PS*PS*TPC-OH
24	IgA-Pep07	H_2N-KTPPTPSPSTPC-OH
25	IgA-Pep08	H_2N-KTPPTPSPST*PC-OH
26	IgA-Pep09	H_2N-KPT*PS*PS*TPPT*C-OH
27	IgA-Pep10	H_2N-KPSPSTPPTPSC-OH
28	IgA-Pep11	H_2N-KPS*PS*TPPT*PSC-OH
29	IgA-Pep12	H_2N-KPSTPPTPSPSC-OH
30	IgA-Pep13	H_2N-KPS*TPPT*PSPSC-OH
31	IgA-Pep14	H_2N-KPSTPPTPSPSC-OH
32	IgA-Pep15	H_2N-KPST*PPTPS*PS*C-OH
33	IgA-Pep16	H_2N-KPSTPPTPS*PSC-OH
34	IgA-Pep17	H_2N-KPSTPPTPSPS*C-OH
35	IgA-Pep18	H_2N-KPST*PPTPSPSC-OH
36	Mannose5 (Man5)	
37	Lacto-*N*-neo-tetraose (LNnT)	
38	Blood group A tetraose	
39	Blood group A pentaose	

sequences resembling the Tn(+)IgA1 glycopeptides. We did not observe binding to any glycans with terminal GalNAc, which suggests that the anti-Tn antibodies do not bind to glycans simply expressing terminal GalNAc (fig. S3D). These data indicate that anti-Tn antibodies in sera are predominantly of IgM subclass that is consistent with Fig. 1B and that these antibodies bind to modeled glycopeptides based on Tn(+)IgA1.

In addition, to more directly demonstrate specific binding of anti-Tn antibodies to Tn(+)IgA1, we took advantage of the fact that the human

Dakiki B cell line secretes IgA1 (*17*). Using the CRISPR-Cas9 system, we deleted the X-linked *Cosmc* (*C1GalT1C1*) gene, thus creating a *Cosmc*KO (*Cosmc*-knockout) B cell line that is unable to generate complex *O*-glycans and can only synthesize the Tn antigen on IgA1 and all other glycoproteins (fig. S4, A to E). *Cosmc* encodes the key molecular chaperone that regulates formation of active T-synthase, required for generating core 1 *O*-glycans and all further extended forms (*30*–*33*). We purified the secreted IgA1 from both wild-type (WT) Dakiki cells and *Cosmc*KO B cells. SDS-PAGE immunoblot analysis of the purified IgA1 shows that the KO cell line produces the Tn(+)IgA1 glycoform, as predicted, which is recognizable by the lectin *Vicia villosa* agglutinin (VVA) and anti-Tn antibodies from human sera. By contrast, normal WT-IgA1 [Tn(−)IgA1 glycoform] lacks the Tn antigen and is not bound by reagents that bind the Tn antigen (Fig. 1G). We then questioned whether Tn(+)IgA1 could inhibit binding of affinity-purified anti-Tn antibodies to the Tn glycopeptide array, as observed in Fig. 1 (D and E). These results demonstrate that Tn(+)IgA1, but not WT-IgA1, can inhibit the binding of the anti-Tn antibodies to the Tn glycopeptide array (Fig. 1H). Together, the results demonstrate that anti-Tn IgM antibodies can specifically interact with Tn(+)IgA1.

Elevated level of anti-Tn antibodies in sera of patients with IgAN

With these tools in hand, we measured the level of anti-Tn antibodies in sera from patients with IgAN compared to healthy controls. Because affinity-purified anti-Tn antibodies contain predominantly the IgM subclass (Fig. 1B), we focused measurements on the levels of anti-Tn IgM. We established a highly sensitive flow cytometric assay that uses high-density conjugation of Asialo-BSM to microbeads (Fig. 2A). We created a standard titration curve using purified anti-Tn IgM from healthy sera (Fig. 2B). Using this curve, we measured a relatively high level of anti-Tn IgM in serum from patients with IgAN (2.2 to 10.6% of total IgM), as compared to control sera (0.8 to 2.7% of total IgM). There were no significant differences in total serum IgM in control versus IgAN samples (Fig. 2C). SDS-PAGE immunoblots probed for IgM, IgG, and IgA of the purified anti-Tn antibodies showed consistent results, demonstrating elevations of IgM to the Tn antigen (Fig. 2D). In addition, we measured the titer of serum IgA1 levels and

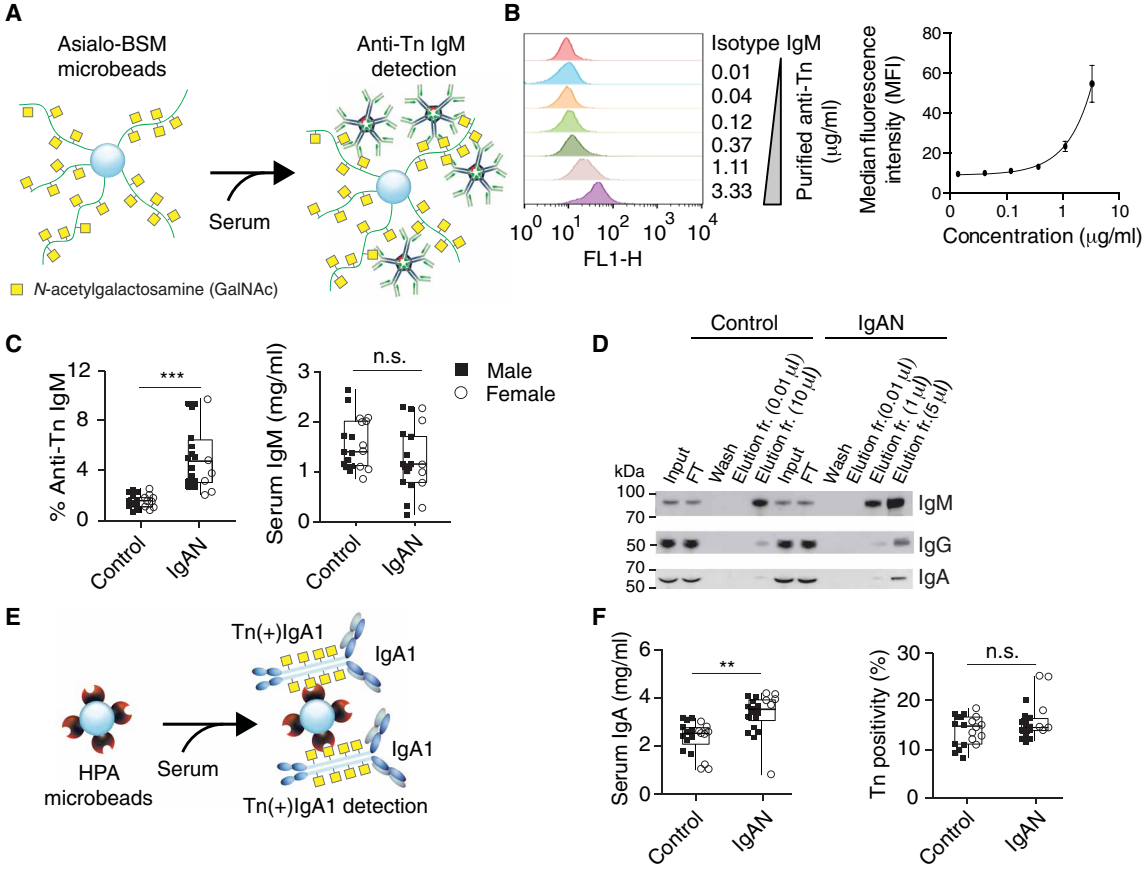

Fig. 2. Elevated level of anti-Tn antibodies and total IgA1 in patients with IgAN. (**A**) Depiction of anti-Tn IgM detection directly from human sera using Asialo-BSM microbeads, similar to Tn(+)matrix beads in fig. S1A, flow cytometry using Alexa Fluor 488–labeled anti-human IgM for signal detection. (**B**) Plot of standard curve of purified anti-Tn IgM from human sera and isotype human IgM serves as a control. (**C**) Sera with IgAN (P1 to P20) or control (C1 to C20) analyzed by flow cytometry using Asialo-BSM microbeads. Donor information listed in Table 1. Serum IgM analyzed using enzyme-linked immunosorbent assay (ELISA). Box plot represents three independent experiments (control, $n = 20$; IgAN, $n = 20$; ■, male; ○, female). Student's t test, $^{***}P = 1.3 \times 10^{-06}$; n.s. (not significant), $P = 0.07$. (**D**) Affinity-purified anti-Tn antibodies of parallel experiments, as in Fig. 1A, from healthy control (C2) and patient with IgAN (P1) were loaded as indicated on top of the immunoblots, and immunoblots were probed for IgM, IgG, and IgA antibodies as indicated on the right. (**E**) Depiction of Tn(+)IgA1 detection from human serum using HPA microbeads by flow cytometry using fluorescein isothiocyanate (FITC)–labeled anti-human IgA1 for signal detection. (**F**) Sera with IgAN (P1 to P20) or control (C1 to C20) were analyzed by flow cytometry using HPA microbeads. Purified Tn(+)IgA1 and Tn(−)IgA1 were used as 100 and 0%, respectively. Serum IgA was analyzed using ELISA. Box plots represent three independent experiments (control, $n = 20$; IgAN, $n = 20$; ■, male; ○, female). Student's t test, $^{**}P = 2.0 \times 10^{-04}$; n.s., $P = 0.10$.

its percentage of Tn positivity using *Helix pomatia* agglutinin (HPA) microbeads (Fig. 2E). Serum IgA1 levels were elevated in patients with IgAN as compared to healthy controls as expected (Fig. 2F, left), but the percentage of Tn positivity of IgA1 in serum did not change in both groups (Fig. 2F, right), suggesting an increased amounts of Tn(+) IgA1 in the circulation of the patient with IgAN. These data indicate that the levels of both anti-Tn antibodies and Tn(+)IgA1 tend to be higher in sera of patients with IgAN compared to sera of controls, thus potentially contributing to enhanced formation of IgM and IgA1 ICs.

Characterization of circulating macromolecular anti-Tn CICs purified from human sera

The above results collectively suggest the possibility of CICs composed of IgM and Tn(+)IgA1 (Figs. 1, B and D to H, and 2D). To explore this possibility, we used a blue native–agarose PAGE (BN-APAGE) system, which resolves native protein complexes up to 6 MDa or more (*34*). First, using the Tn(+)matrix, we affinity-purified anti-Tn antibodies from control sera and sera from patients (P1, P3, and P4) and used the BN-APAGE system to resolve the bound materials; the resulting immunoblots were then probed for IgM. The results revealed that IgM-containing anti-Tn CICs migrated predominantly as large–molecular weight species of 1.2 MDa and above, with substantially higher–molecular weight species (several megadaltons) than control IgM, which migrated at the expected size of ~0.9 MDa (Fig. 3A). As a control IgM, we used ReBaGs6, which is a recombinant anti-Tn mouse IgM that binds to Tn(+)matrix (*35*). This control antibody was purified using a similar approach on the Tn(+)matrix; the bound ReBaGs6 IgM had a predicted normal size when resolved on BN-APAGE, demonstrating that no artificial complexes are formed by possible leakage of Asialo-BSM from the Tn(+)matrix (Fig. 3B). In parallel, we used BN-APAGE to analyze the sizes of affinity-purified anti-Tn antibodies and total IgM (similar concentration used as in Fig. 3A) from controls (C2, C3, and C6). These CICs also showed similar behavior of anti-Tn IgM ICs from patients (Fig. 3C), indicating that the ICs from both healthy controls and patients appear to be similar at least in terms of apparent mass but differ as shown above in total levels, being higher in patient sera. We did not observe any anti-Tn IgM antibody similar to the size of pentameric IgM in both healthy and patients with IgAN (Fig. 3, A and C), suggesting that the anti-Tn IgM is associated with other molecules, possibly IgA1 and/or IgG, as these were observed also in the original Tn(+)matrix-bound materials (Fig. 1B), along with possibly other serum glycoproteins. In similar analyses of the purified anti-Tn CICs from patients with IgAN, as defined in Fig. 1B, we observed three to four distinguishable bands in patients with IgAN, potentially representing IgM, IgG, and Tn(+)IgA1 (Fig. 3D). As controls, we also analyzed total sera from both healthy control and IgAN cases using BN-APAGE system, probed for total IgM, IgG, and IgA, and did not observe higher–molecular weight complexes under these conditions, which suggests that CICs are a relatively small component of overall sera (fig. S5, A to C). Together, these data indicate that CICs of megadalton size could potentially contain all of the components that account for complexes in the megadalton mass. However, even the smallest CICs would be predicted to contain at least IgM and one or more of IgA and/or IgG.

Anti-Tn CICs contain IgM and IgA1, and the Tn antigen–based glycomimetics disrupt CICs

The above results do not exclude the possibility that Tn(+)IgA1 could be confined only to one complex or may not be present at all within the anti-Tn IgM complexes. To examine the distribution of the Tn(+)IgA1 within the large anti-Tn CICs containing IgM (Fig. 3, A, C and D), we immunodepleted the anti-Tn CICs using anti-IgA and control antibodies and observed specific codepletion of IgM with IgA (Fig. 3E, middle lane). This result is consistent with the prediction that IgM and IgA are associated with each other within the complexes.

Furthermore, we tested whether the anti-Tn IgM ICs can be dissociated from Tn(+)IgA1 using compounds that mimic the Tn antigen–based glycomimetics. For this purpose, we affinity-purified anti-Tn CICs from the sera of patients with IgAN; the anti-Tn CICs were treated with mock, α-methylGalNAc (glycomimetic compound, αGalNAc), or α-methylGlcNAc (control compound, αGlcNAc), followed by BN-APAGE Western blot (WB) and probing for IgM and IgA. Only α-methylGalNAc, but not the control α-methylGlcNAc, caused dissociation of the Tn(+)IgA1 from anti-Tn IgM ICs (Fig. 3F, bottom, lane 2), releasing Tn(+)IgA1, which had a similar electrophoretic mobility to control native IgA1 (Fig. 3F, bottom, lanes 4 and 5). We were unable to detect an IgA1 signal in mock and α-methylGlcNAc–treated samples (Fig. 3F, bottom, lanes 1 and 3), indicating that the IgA1 epitopes may be buried within the CICs and thus not available in this native page setup for WB detection.

Next, we analyzed the efficacy of α-methylGalNAc to block binding of anti-Tn IgM, which could be used to prevent the formation of the macromolecular anti-Tn CICs, because anti-Tn IgM complexes have available Tn antigens sites and the IgM within binds to both Tn-containing IgA1 glycopeptides and intact IgA1 (Fig. 1, D to H). Upon analysis using the Tn glycopeptide array, as in Fig. 1, α-methylGalNAc specifically inhibited binding of the anti-Tn IgM (Fig. 3G). We further synthesized a dimeric version of the Tn antigen, termed DiαGalNAc (i.e., GalNAc dimer) along with a control DiαGlcNAc (i.e., GlcNAc dimer) (figs. S6 to S13). The DiαGalNAc exhibited higher inhibition compared to α-methylGalNAc in terms of anti-Tn antibody binding to the array, as listed (Table 2 and fig. S14A). Furthermore, we calculated the median inhibitory concentration (IC_{50}) values using an enzyme-linked immunosorbent assay (ELISA)–based approach, where we used Tn glycopeptides from IgA1 (IDs 18 and 19; listed in Table 2), and performed the inhibition experiments using the glycomimetics (i.e., α-methylGalNAc and DiαGalNAc). We observed higher inhibition of anti-Tn CICs binding with DiαGalNAc treatment (fig. S14, B and C). Together, the result indicates that the anti-Tn CICs are composed of at least IgM and IgA and Tn antigen glycomimetics specifically dissociate Tn(+)IgA1 from the complexes.

Glycomimetic treatment inhibits the proliferative nature of anti-Tn CICs on primary human mesangial cells

Several studies suggest that ICs containing Tn(+)IgA1 from patients with IgAN stimulate mesangial cell proliferation (*36*–*38*). We therefore analyzed whether the purified anti-Tn CICs have bioactivity toward mesangial cells. First, we analyzed the binding nature of anti-Tn CICs to mesangial cells. For this, the cultured cells were fixed, permeabilized with 0.05% Triton X-100, and stained with anti-Tn CICs. We found that anti-Tn CICs from both patient with IgAN and healthy control bind to the cells, whereas isotype control antibodies do not bind (Fig. 4, A to C); this is consistent with the characteristics of autoantibodies. Furthermore, we also analyzed anti-Tn CICs binding to mesangial cell surfaces, using flow cytometric analysis; we stained the cells with anti-Tn CICs and analyzed the binding, and we observed significant binding not only with the predominant component of anti-Tn CICs (IgM) but also with IgA1

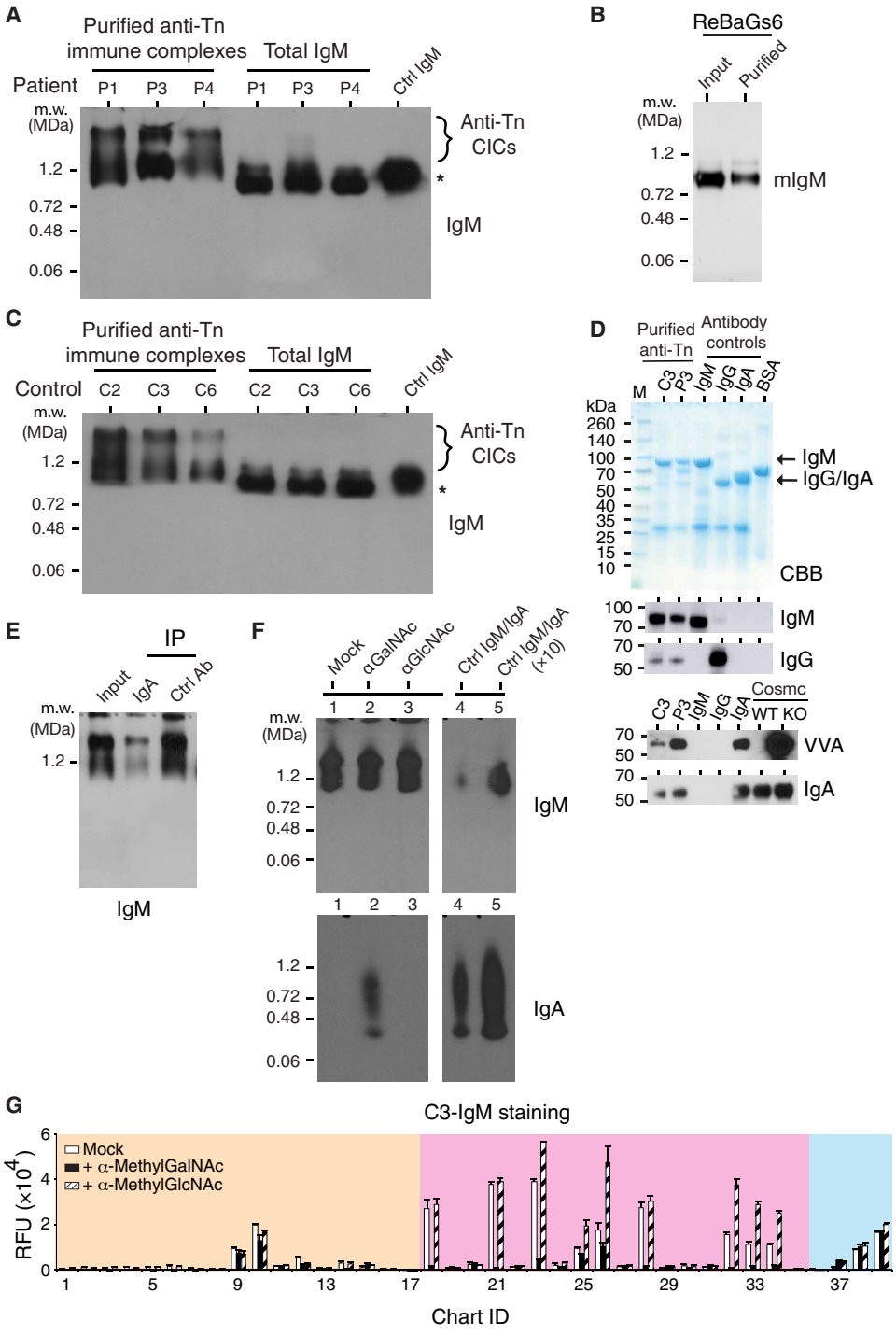

Fig. 3. Identification of anti-Tn CICs in sera of patients with IgAN and healthy controls sera and complexes dissociate with glycomimetic. (**A**) BN-APAGE analysis of Tn(+)matrix affinity purified anti-Tn antibodies and total purified IgM. Left: Native molecular weight markers for approximation of molecular weight (m.w.). P1, P3, and P4 represent three patients; control IgM. (**B**) Tn(+)matrix affinity-purified ReBaGs6 antibody resolved by BN-APAGE system and blotted for murine IgM. (**C**) Similar to (A), BN-APAGE analysis of affinity-purified anti-Tn antibodies and total purified IgM from three healthy controls (C2, C3, and C6) and control IgM immunoblotted for IgM. (**D**) Coomassie-stained SDS-PAGE gel of affinity-purified anti-Tn antibodies from healthy control (C3) and patient (P3); control antibodies and BSA as indicated. Immunoblots (bottom) of same preparation probed as indicated. VVA and IgA blots performed with appropriate controls: purified Tn(+)IgA1 and Tn(−)IgA1 produced from *Cosmc*KO and WT Dakiki cells, respectively. (**E**) Anti-Tn CICs purified from serum of patients with IgAN immunodepleted with anti-IgA or isotype control antibodies (Ab); depleted materials analyzed by BN-APAGE WB probed for IgM. IP, immunoprecipitation. (**F**) Anti-Tn CICs purified from serum of patient with IgAN treated with mock, α-methylGalNAc (αGalNAc), or α-methylGlcNAc (αGlcNAc); samples analyzed by BN-APAGE WB and probed for IgM and IgA. (**G**) Tn glycopeptide array probed with anti-Tn antibodies (C3) preincubated with 20 mM α-methylGalNAc or 20 mM α-methylGlcNAc and stained with Alexa Fluor 488–labeled anti-human IgM. Error bars represent ±1 SD of four replicates. $n = 3$ except blot images from (A), (C), and (E); $n = 2$. Asterisk represents normal pentameric IgM.

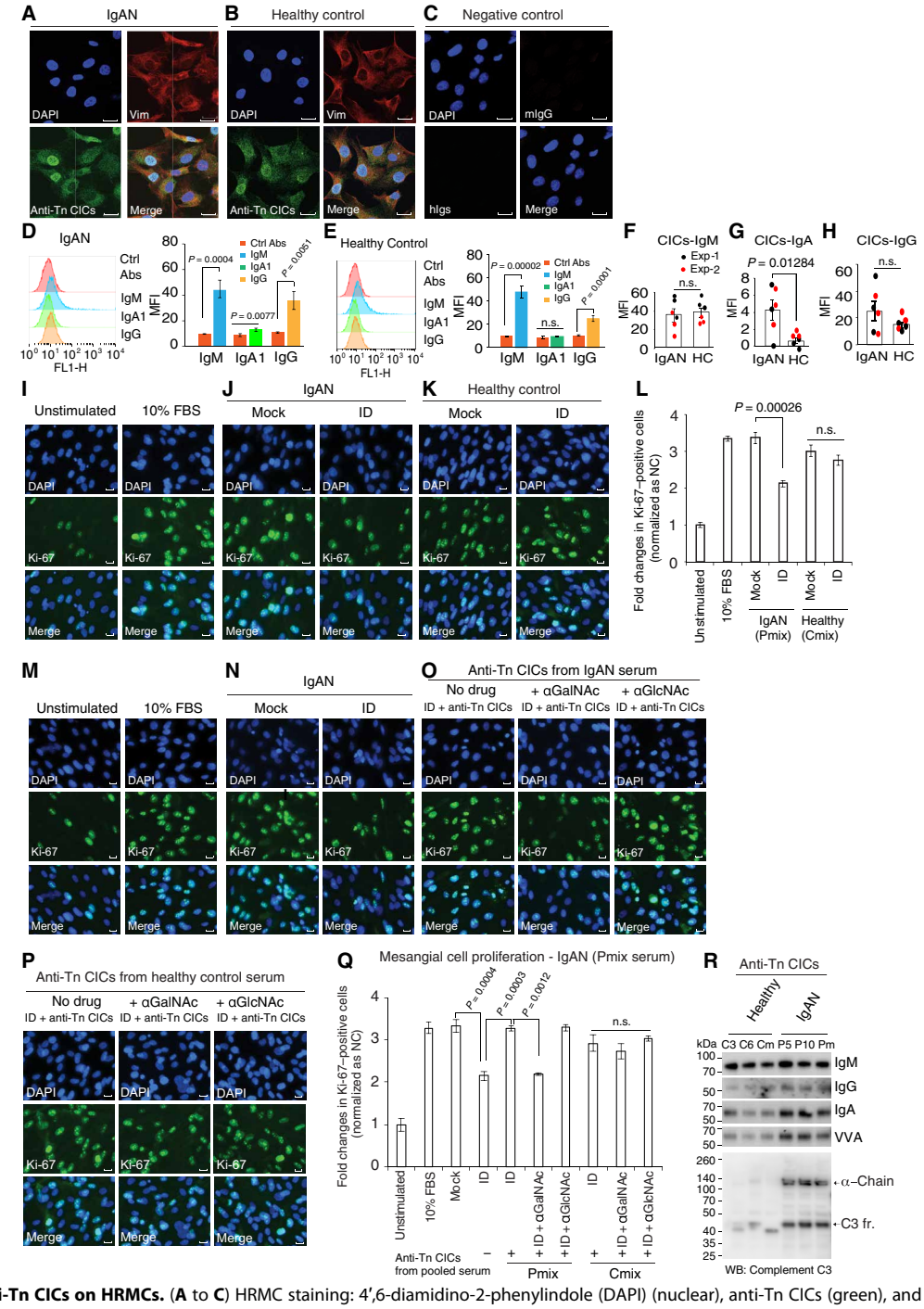

Fig. 4. Activity of anti-Tn CICs on HRMCs. (**A** to **C**) HRMC staining: 4′,6-diamidino-2-phenylindole (DAPI) (nuclear), anti-Tn CICs (green), and vimentin (red); negative control (mixture of isotypes IgM, IgG, and IgA). Experiments performed on three patients with IgAN (P5, P10 and Pmix) three healthy controls (HC) (C3, C6, and Cmix), representative example. (**D** and **E**) Surface staining by anti-Tn CICs. HRMCs stained with anti-Tn CICs purified from IgAN (P5, P10, and Pmix) or healthy controls (C3, C6, and Cmix), probed as indicated. Right: The respective mean fluorescent intensity (MFI) for each antibody is plotted against the control. Error bars represent ±SEM ($n = 6$, two independent experiments of $n = 3$). (**F** to **H**) MFI from (D) and (E) plotted ($n = 6$, two independent experiments of $n = 3$); black and red circles, individual cases; bar, average. (**I** to **L**) Proliferation of anti-Tn CICs on starved HRMCs. (I) Unstimulated [0.5% fetal bovine serum (FBS)] and stimulated (10% FBS); HRMCs stimulated using IgAN serum (J) (Pmix) or healthy control (K) (Cmix) where anti-Tn CICs immunodepleted using Tn(+)matrix beads (ID) or mock. Ki-67, cell proliferation marker (green); DAPI, nuclear staining (blue). (L) Quantification of (I) to (K): error bars, triplicates measure (three areas per well). NC, negative control (unstimulated). (**M** to **Q**) Exogenous addition of purified anti-Tn CICs stimulates HRMCs, and glycomimetic inhibits proliferation. (M, N) Similar to I and J. (O and P) Exogenous addition of anti-Tn CICs (50 ng/100 ml per well) purified from IgAN patient or healthy control to Tn(+)matrix depleted sera from patient with IgAN, with/without prior treatment of anti-Tn CICs with α-methylGalNAc or α-methylGlcNAc. Scale bars, 20 μm. (Q) Quantification of (M) to (P), fold change of Ki-67–positive cells normalized to unstimulated. Error bars, triplicate measure (three areas per well). Representative of three biological replicates, IgAN and healthy control. (**R**) Purified anti-Tn CICs from three healthy controls and three patients with IgAN resolved by SDS-PAGE WB, probed as indicated ($n = 3$, technical replicates). Cm, Cmix; Pm, Pmix.

and IgG (Fig. 4, D and E) to mesangial cells (except IgA1 in the case of healthy control), indicating that anti-Tn CICs can interact with the mesangial cell surface. We also asked whether there is any difference in anti-Tn CICs, purified from sera of patients with IgAN and healthy controls, binding to mesangial cells, and our analysis showed that there is no difference in binding except in the case of IgA1 (Fig. 4, F to H).

To investigate the proliferative nature of the anti-Tn CICs, we directly used sera from both patients with IgAN and healthy controls to stimulate primary mesangial cells, which were cultured under 0.5% fetal bovine serum (FBS)–containing medium, directly stimulated the cells with different concentrations of the serum, and then stained for the proliferation marker Ki-67. Results using stained cells were calculated as a fold change. We found that both sources of sera stimulate mesangial cells in a dose-dependent manner, but stimulation by sera from patients with IgAN was significantly higher than healthy controls, and the difference was more evident in lower serum concentrations (1 and 2.5%); at 5%, the difference was not significant, perhaps because of saturation (fig. S15, A and B). There were no obvious changes observed in total serum protein with IgAN compared to healthy controls (fig. S15 C). Next, we immunodepleted anti-Tn CICs with the Tn(+)matrix or mock using the sera from both patients with IgAN and healthy controls; the immunodepleted sera were added to cells and stained for Ki-67. The results demonstrate that the depletion of anti-Tn CICs from sera of patient with IgAN significantly reduces its proliferative nature of the mesangial cells compared to mock depletion (Fig. 4, I, J, and L, mock and ID in Pmix), indicating that anti-Tn CICs are bioactive. In parallel experiments with healthy control sera, we did not see significant changes in proliferative nature of the sera depleted of anti-Tn CICs (Fig. 4, I, K and L, mock and ID in Cmix), which may also be due to the significantly lower amount of anti-Tn CICs and potential differences in the components of the CICs in the sera of healthy controls as compared to those in patients with IgAN (Fig. 2C).

Nevertheless, to further explore the biological activity of the anti-Tn CICs purified from both patient with IgAN and healthy controls on mesangial cells, we purified the anti-Tn CICs from both sources. Similar to Fig. 4 (I and J), we prepared cultured cells with immunodepleted IgAN serum, and then we stimulated the cells by adding the same amount of anti-Tn CICs purified either from IgAN sera or from the healthy control sera; for the specificity, we tested human embryonic kidney (HEK) 293T cells, in parallel with HRMCs, as a control cell line for the cell proliferation assay. We found that anti-Tn CICs do not stimulate HEK293T cells (fig. S16, A and B). The results demonstrate that the anti-Tn CICs from both IgAN and the control serum stimulate the cells as seen by Ki-67 staining (Fig. 4, M to Q, ID and ID + anti-Tn CICs). We again asked whether α-methylGalNAc, which dissociates the anti-Tn CICs from patient with IgAN (Fig. 3F), could inhibit the proliferative activity of the anti-Tn CICs. The result demonstrates that the pretreatment of the anti-Tn CICs purified from patients with IgAN with α-methylGalNAc inhibits their proliferative activity toward mesangial cells; in parallel control experiments, the control compound α-methylGlcNAc did not inhibit the mesangial cell proliferation as expected (Fig. 4, O and Q). The use of similarly α-methylGalNAc pretreated anti-Tn CICs purified from healthy control sera did not significantly inhibit mesangial cell proliferation (Fig. 4, P and Q). Together, the results demonstrate that the purified anti-Tn CICs, irrespective of IgAN status, can stimulate mesangial cell proliferation and that the glycomimetics specifically inhibit the stimulatory nature of only anti-Tn CICs purified from patients with IgAN.

Prior studies suggest that complement plays an important role in IgAN pathogenesis and IgA1-containing CICs have been observed with complement C3, one of the components of the complement pathway. It has been reported that complement can be activated within the CICs in circulation or after the ICs being deposited to glomerular mesangium (*39*–*41*, *42*). Our MS analysis of the anti-Tn CICs purified from healthy control sera demonstrated the presence of complement C3 (fig. S2 and table S1). To better understand the presence of complement C3 within the purified anti-Tn CICs from patients with IgAN, we purified CICs from sera of both healthy control and patient with IgAN and analyzed the materials by SDS-PAGE immunoblots. Purified anti-Tn CICs from sera of patients with IgAN contain IgM, IgG, and Tn(+)IgA1 and substantially higher level of complement C3 compared to CICs purified from healthy controls (Fig. 4R). These results indicate that anti-Tn CICs purified from patients with IgAN are different in terms of amounts of complement C3. In addition, the substantially higher amount of complement C3 within anti-Tn CICs may explain the differential mesangial cell proliferation by anti-Tn CICs from IgAN compared to healthy control (Fig. 4, I to Q). Together, anti-Tn CICs that we have purified from serum of patient with IgAN contain IgM, Tn(+)IgA1, IgG, and complement C3, suggesting a pathogenic nature of anti-Tn CICs of patients with IgAN in their serum.

DISCUSSION

Despite many years of study on the CICs responsible for IgAN pathogenesis (*9*, *43*), much remains to be learned about the nature of such complexes. Here, we identified and purified novel anti-Tn CICs of size ranging from ~1.2 MDa to several megadaltons and demonstrate that these ICs consist predominantly of IgM and, to a lesser extent, Tn(+)IgA1 and IgG. These anti-Tn CICs are significantly elevated in the sera of patients with IgAN together with complement C3. Furthermore, these purified anti-Tn CICs specifically stimulate primary HRMCs. Tn antigen glycomimetics can dissociate these anti-Tn CICs to release Tn(+)IgA1 and also inhibit the proliferative nature of the anti-Tn CICs on primary HRMCs. These insights could have enormous potential for drug development to treat and manage IgAN. We also developed a unique assay to detect these anti-Tn CICs directly from serum, which could potentially be used as a much-needed early diagnostic tool for IgAN.

A key focus of our study was to define the identities, properties, and major components of the anti-Tn CICs in human serum, particularly focused on IgAN. A key advantage of our approach was the affinity purification of such complexes using a Tn(+)matrix, which allowed us to identify and quantify the anti-Tn CICs and their ability to bind the Tn(+)IgA1. In addition, a key aspect of our study was the generation of unique glycoforms of IgA1, i.e., Dakiki cell–derived materials with or without *Cosmc* expression representing Tn(−)IgA1 and Tn(+)IgA1, respectively. We succeeded in both of these goals, and the availability of the Tn(+)matrix and Tn(−)IgA1 and Tn(+)IgA1 glycoforms should be very helpful in future studies to determine the interactions of IgA1 with autoantibodies.

We observed that IgM, Tn(+)IgA1, and IgG form CICs of several megadalton sizes, which contain predominantly IgM. There may be other proteins associated with these large molecular masses, based on BN-APAGE size estimation and Coomassie-stained SDS-PAGE bands, while the smaller size of CICs of ~1.2 MDa may contain IgM and few IgA1 molecules. It is not unexpected that the anti-Tn CICs

are heterogeneous in terms of combinations of IgM, Tn(+)IgA1, and IgG as well as other apparent substoichiometric level of proteins present within the complexes. We speculate that IgM directly interacts with the Tn antigen of IgA1 within anti-Tn CICs that we have purified, because both the Tn matrix used for the pull-down and IgA1 itself have the Tn antigen, and the IgM does bind to the Tn antigen. However, we do not yet know whether the anti-Tn CICs that we found deposit in the kidney and are responsible for IgAN pathogenesis, but our hypothesis is that elevated levels of anti-Tn CICs containing predominantly complement C3 deposit in the kidney and promote IgAN pathogenesis. On the other hand, whether such anti-Tn CICs that we have purified are common in patients with IgAN is a very important question that is the subject of our future studies.

Although IgAN is characterized by mesangial deposition of IgA1 with IgG and/or IgM (*2*), there is a lack of information as to whether there is colocalization of Tn(+)IgA1 with either IgG and/or IgM in all types of IgAN deposits. Because of the biochemical nature of our work with a limited number of patients and their serum samples, we were unable to expand our work to a large cohort of patients, so it is not clear at this point whether the inclusion of anti-Tn IgM within anti-Tn CICs is a common characteristic in IgAN or only limited to a small number of patients. However, it has been reported that 4 to 70% of pediatric patients presenting IgAN have mesangial deposits of IgM (*44*). Such IgM deposition showed a significant association with glomerular crescent, mesangial hypercellularity, segmental sclerosis, and tubular atrophy/intestinal fibrosis (*45*). A similar study that focused on IgM identified IgM antibody deposits in the glomerulus, along with a similar distribution of IgA1 in a specimen from a patient with IgAN (*46*). There are many other studies examining individual antibody levels (IgG, IgM, and IgA1) or some combinations of them, suggesting their deposition in the kidney of the patients with IgAN or in a mouse model (*47*–*51*). On the other hand, a recent study using confocal microscopy on frozen kidney-biopsy specimens, along with other biochemical approaches, observed colocalization of IgG and IgA, thus suggesting a potential colocalization between Tn(+)IgA1 with IgG, but that study did not describe potential IgM colocalization (*52*). Surprisingly, many studies in the field have focused on IgA1 but not specifically Tn(+)IgA1, which is the predicted antigen, nor the glycosylation of these antigenic IgA1 glycoforms in deposits has been well characterized chemically. Cumulatively, to determine the importance of anti-Tn CICs in IgAN pathogenesis, a longitudinal clinical study focused on a large cohort of human patients designed to study IgM deposition and disease activity should be considered. These are likely to be topics of future studies.

Our results demonstrate that the anti-Tn CICs purified from the healthy controls, although present at lower levels in serum, compared to patients, bind to and can stimulate primary HRMCs to a similar level equivalently to ICs purified from a patient with IgAN when tested under similar concentrations. However, a major difference in this activity that we observed is their relationship upon treatment with glycomimetics. For example, unlike anti-Tn CICs purified from healthy controls, the CICs purified from patients with IgAN failed to stimulate HRMCs when pretreated with α-methylGalNAc that can cause dissociation of the CICs. This indicates possible differences between the ICs purified from healthy control and patients in relation to composition, stoichiometry, and specificity within the components. One of the major differences that we found is the predominant presence of complement C3, but to gain a deeper understanding of the role of C3 within anti-Tn CICs will require further study at the native macromolecular complexes, proteomic, and compositional levels. It is possible that the components of anti-Tn CICs in the sera of patients with IgAN may have reorganized toward low-affinity ICs together with higher accessibility of the glycomimetic. Such future studies will define the components of the complexes and further characterize IgM and Tn(+)IgA1 within the complexes. In addition, our results indicate that the anti-Tn CICs both from patients with IgAN and healthy controls bind to HRMCs preferentially, as well as to their nuclei. Binding to the nuclei is puzzling and will require further studies as to whether the CICs also contain antinuclear antibodies or whether the Tn-containing antigens may somewhat reside within cells, as has been proposed by others (*53*). Such a finding might have implications for IgAN pathogenesis.

We envision that increased levels of circulating Tn(+)IgA1 together with the broad exposure of Tn antigens by various sources, for example, microorganisms and parasitic infections during childhood and beyond with organisms expressing the Tn antigen, could lead to the development of anti-Tn antibodies (particularly IgM) (*17*, *21*, *25*, *54*). In addition, some population-based genome-wide association studies have indicated nearly 20 IgAN risk loci (*55*); moreover, in a similar study, locus 7p21.3 (*C1GALT1*, *T-synthase*; the enzyme that is important in generating extended *O*-glycans) and locus Xq24 (*C1GALT1C1*, *Cosmc*; the specific molecular chaperone for T-synthase) are associated with serum Gd-IgA1 levels (*30*, *32*, *56*, *57*). Consistent with these studies, defects in *Cosmc* and *T-synthase*, in IgA1-producing B cells have been suggested to be responsible for generating the Tn glycoform (*58*–*61*), but studies in this area are continuing (*57*, *62*–*64*). Thus, consistent with the multihit hypothesis as to the origin of IgAN, the presence and elicitation of anti-Tn IgM antibodies along with generation of the Tn(+)IgA1 create the background by which IgAN may arise.

The anti-Tn CICs that we have purified from human serum show many biochemical and biological characteristics similar to prior characterize CICs and align with evolving model of CICs known to be important in IgAN pathogenesis (*8*, *9*, *26*, *65*). Our data unequivocally demonstrate that anti-Tn CICs that we have purified contain galactose-deficient IgA1 as the key component together with IgM; these complexes may also contain some IgG. Tn antigen–based glycomimetics treatment followed by blue native gel analysis shows the presence of polymeric IgA1 within the complexes. Purified anti-Tn CICs from healthy control can bind to and stimulate proliferation of HRMCs; such occasional IgA1 deposition may occur as seen in healthy kidney biopsies (*66*, *67*), and the interactions may be different or not sufficient to cause IgAN pathogenesis. For sera from patients with IgAN, our results show that anti-Tn CICs are elevated and that complement C3 is elevated within the ICs compared to anti-Tn CICs found in healthy control sera; such differences may be critical for driving IgAN pathogenesis. However, we do not yet know whether the anti-Tn CICs that we have found deposit in the kidney and are specifically responsible for IgAN pathogenesis, but our hypothesis is that elevated levels of anti-Tn CICs containing predominantly complement C3 deposit in the kidney and promote IgAN pathogenesis. Establishing the relevance of anti-Tn CICs to IgAN is important, which is part of ongoing work.

Another important aspect of our study is the development of a sensitive assay to detect and monitor anti-Tn IgM antibodies in circulation, which has important implications for IgAN diagnosis and as a tool to follow disease progression. We have developed an assay on the basis of our findings that IgM is dominantly present within

the anti-Tn CICs, which contain IgM and IgA1 together. Our work shows that IgM within the CICs can be easily detected by secondary anti-IgM antibodies, whereas IgA1 and IgG cannot be directly and easily detected in the native CICs. Hence, we reasoned that an assay targeted toward detecting IgM bound to the Tn(+)matrix would be more meaningful and sensitive. Accordingly, using this tool, we were able to measure significant levels of anti-Tn CICs in the sera of patients with IgAN as compared to healthy control sera. Many IgAN diagnostic platforms have focused their efforts on detecting primarily IgA1-IgG, complement C3 and, in very few instances, IgA1-IgM ICs. Future studies should take into account the dominant presence of IgM within the CICs together with other antibodies and complement C3.

Despite many years of studies since the original description of the IgAN (*1*) and progress made for nonspecific inhibition of the renin-angiotensin aldosterone system and steroids for patients, there is no specific therapy for this disease (*47*). Our insights into the carbohydrate-protein interactions within the CICs led us to test a new class of small-molecule glycomimetics (*68*). We found that the α-methylGalNAc–based glycomimetics can dissociate the purified anti-Tn CICs into IgA1 and IgM. On the other hand, they also prevent the interaction of the purified anti-Tn antibodies with Tn-containing IgA1 glycopeptides, suggesting that they can potentially block the formation of the CICs. Cumulatively, glycomimetics represent promising candidates to consider for the treatment of IgAN. It has been reported that the properties of CICs (Tn-containing IgA1), for example, size, components, and antigen:antibody ratio, influence the nature of the CICs deposited in the glomeruli (*69*, *70*). Thus, we imagine that the anti-Tn CICs that we purified behave similarly and that treatment of the anti-Tn CICs with α-methylGalNAc–based glycomimetics can dissociate the Tn(+)IgA1 from the complex and reduce kidney deposition. Such glycomimetics may hold great potential for treatment of patients if the compounds are orally administrable and absorbable. Such possibilities are reasonable, as simple sugar compounds are used to treat other diseases, such as the use of oral fucose or mannose supplements to treat congenital disorders of glycosylation (*71*, *72*–*76*). The glycomimetics, if accessible and stable in the circulation, could be effective in disrupting anti-Tn ICs.

MATERIALS AND METHODS

Serum collection

Blood samples from patients with IgAN, biopsy-proven, were obtained either from the Emory Clinic under the approved Institutional Review Board (IRB) protocol (IRB00008410) as previously described (*17*) or from the VU University Medical Center (VUMC) Amsterdam, The Netherlands, approved by both the patients and by the Medical Ethical Committee of the hospital (METC-VUMC) under approved Central Committee on Research Involving Human Subjects (CCMO) (NL12328.029.06). Blood samples for healthy donors were obtained from Beth Israel Deaconess Medical Center under the approved IRB protocol (2016P000008) and from the VUMC Amsterdam, under approved CCMO (NL12328.029.06). In addition, basic donor information is listed in Table 1. Collected blood samples were kept at room temperature (RT) (1 hour) and centrifuged (2000 rpm) for 10 min at RT; the resultant supernatants were collected as serum.

Preparation of Tn(+)matrix affinity resin

We prepared Tn(+)matrix [desialylated BSM (Asialo-BSM)] resins as previously described (*35*). Briefly, ~2 ml of coupled BSM resins (50% slurry) were desialylated using 50 mU of neuraminidase (catalog no. 10269611001, Roche) in 50 mM sodium acetate (pH 5.0) for 1 hour at 37°C (10 rpm). The beads were washed three times with 10 ml of phosphate-buffered saline (PBS) and desialylated one more time to completely remove the remaining sialic acid. The prepared Asialo-BSM beads [Tn(+)matrix beads] were kept at 4°C in PBS for future uses. Beads alone were prepared with no proteins in parallel.

Affinity purification of putative anti-Tn antibodies and WB

Human serum (~50 ml) was mixed with 1 ml of Tn(+)matrix beads (50% slurry in PBS) at 4°C (10 rpm) overnight. The preparation of Tn(+)matrix beads was washed six times with 5 ml of chilled 1 M NaCl on a column (catalog no. 10561284, Pierce) dropwise (1 ml/min), the bound material was eluted by 5 ml of chilled 0.1 M glycine-NaOH (pH 10.5), and eluted sample was immediately neutralized with chilled glycine-HCl. Eluted fraction (6 ml) was dialyzed in 1 liter of PBS using Slide-A-Lyzer Dialysis cassettes (10,000 molecular weight cutoff, 12 ml; Thermo Fisher Scientific) overnight at 4°C and concentrated using Amicon Ultra Centrifugal Filters (10,000 nominal molecular weight limit; catalog no. UFC801096, MilliporeSigma) down to 0.5 ml. The concentration of eluted protein was determined by Bicinchoninic acid assay (catalog no. 23225, Thermo Fisher Scientific). Each fraction (input, flow through, and washes) was proportionally loaded, except elution of 10 μl, analyzed on SDS-PAGE, and stained with Coomassie or transferred to nitrocellulose membrane (catalog no. 1704158, Bio-Rad) using Trans-Blot Turbo Transfer System (Bio-Rad). After blocking with 5% (w/v) nonfat milk (catalog no. C701K28, EMD Millipore) in TBST [50 mM tris-HCl (pH 7.4), 150 mM NaCl, and 0.05% Tween 20] for 1 hour at RT, the membranes were incubated with horseradish peroxidase (HRP)–labeled goat anti-human IgM (μ chain) (catalog no. 5220-0328, KPL), goat anti-human IgG (H+L) (catalog no. 109-005-003, Jackson ImmunoResearch Laboratories Inc.), or goat anti-human IgA (α chain) (catalog no. 5220-0360, KPL) antibodies at 1:10,000 dilution in TBST containing 1% nonfat milk for 1 hour at RT. After washing three times with TBST for 10 min, the signals were analyzed on an Amersham Imager 600 (GE Healthcare Life Sciences) using SuperSignal West Pico chemiluminescent substrate (catalog no. 34578, Thermo Fisher Scientific). For lectin blot, the membranes were blocked with 5% (w/v) bovine serum albumin (BSA) (catalog no. BP1600-1, Fraction V, Fisher BioReagents) in TBST for 1 hour at RT and incubated with biotinylated VVA (catalog no. B-1235-2, Vector Laboratories; diluted to 0.5 μg/ml) in TBST containing 0.5% BSA for 1 hour at RT. HRP-labeled streptavidin (catalog no. SA-5014, Vector Laboratories) at 1:10,000 dilution in TBST containing 0.5% BSA was used for detection.

Immunofluorescence of Tn(+)matrix beads

Tn(+)matrix beads (5 μl; 50% slurry in PBS) or control beads were incubated with purified anti-Tn antibodies diluted to 1 μg/ml for IgM staining and to 4 μg/ml for IgG and IgA staining in PBS for 1 hour on ice. The beads were washed three times with 1 ml of chilled 1 M NaCl each time using centrifugation at 150*g* for 30 s at 4°C and incubated with respective Alexa Fluor 488–labeled goat anti-human IgM (catalog no. A-21215, Thermo Fisher Scientific), goat anti-human IgG (catalog no. A-11013, Thermo Fisher Scientific), or fluorescein isothiocyanate (FITC)–labeled mouse anti-human IgA1 (catalog no. 9130-02, SouthernBiotech) at 1:400 dilution in PBS for 1 hour on ice in the dark. The beads were washed twice with 1 ml of

chilled PBS and analyzed using a microscope (AMG EVOS FL digital inverted microscope, Thermo Fisher Scientific; ×100 magnification). Isotype human IgM (catalog no. 31146; diluted to 1 μg/ml), human IgG (catalog no. 31154; diluted to 4 μg/ml), or human IgA (catalog no. 31148; diluted to 4 μg/ml) from Invitrogen in PBS was used as control. For inhibition assay, purified anti-Tn antibodies were preincubated with 20 mM α-methylGalNAc (catalog no. sc-222088, Santa Cruz Biotechnology) in PBS for 30 min on ice. For additional control experiments, other proteins including BSM, BSA, and fetuin were also coupled independently with beads as described in the "Preparation of Tn(+)matrix affinity resin" section. Beads were incubated with a murine recombinant anti-Tn IgM antibody [ReBaGs6 in house (*35*); diluted to 1 μg/ml], or biotinylated VVA (diluted to 1 μg/ml) in PBS and detected with Alexa Fluor 488–labeled goat anti-mouse IgM (catalog no. A-21042, Thermo Fisher Scientific) or streptavidin (catalog no. S11223, Invitrogen) at 1:400 dilution in PBS. Isotype mouse IgM (catalog no. 0101-01, SouthernBiotech; diluted to 1 μg/ml) in PBS was used as a control.

Tn glycopeptide microarray

The Tn glycopeptide microarray was prepared as previously described (*77*). Briefly, the glycopeptides printed on the microarray is as listed (Table 2). Purified anti-Tn antibodies (diluted to 10 μg/ml for IgM and to 40 μg/ml for IgG and IgA detection) in TSM binding buffer [20 mM tris-HCl (pH 7.4), 150 mM NaCl, 2 mM $CaCl_2$, and 2 mM $MgCl_2$, with 1% BSA and 0.05% Tween 20] were added to the respective array slides for 1 hour at RT. Alexa Fluor 488–labeled goat anti-human IgM or goat anti-human IgG or FITC-labeled goat anti-human IgA antibody at 1:400 dilution in TSM binding buffer was used for detection of IgM, IgG, and IgA within purified anti-Tn antibodies. Slides were analyzed on a Genepix 4300A microarray scanner (Molecular Devices). Images were analyzed with quantitation software (GenePix Pro Microarray Analysis software version 7, Molecular Devices). For inhibition assay, we used purified Tn(+) IgA1 produced from *Cosmc*KO Dakiki cells (see the "Generation and characterization of *Cosmc*KO Dakiki cells using CRISPR-Cas9 system" section) to inhibit anti-Tn antibodies binding to microarray and Tn(−)IgA1 produced from Dakiki cells as a positive control. Purified anti-Tn antibodies (C1; 10 μg/ml) in TSM binding buffer were preincubated with 1 μg of purified Tn(+)IgA1 or Tn(−)IgA1 for 30 min at RT. After 1 hour of incubation with the solution on the array, Alexa Fluor 647–labeled goat anti-human IgM antibody (catalog no. A-21249, Thermo Fisher Scientific; diluted at 1:400) in TSM binding buffer was used for detection. For inhibition assay with glycomimetics, purified anti-Tn antibodies (C3; 10 μg/ml) in TSM binding buffer were preincubated with 20 mM α-methylGalNAc (or α-methylGlcNAc) (catalog no. M0257, Sigma-Aldrich) or DiαGalNAc (or DiαGlcNAc) synthesized as described in the "Synthesis of DiαGalNAc and DiαGlcNAc" section for 30 min at RT; after 1 hour of incubation with the solution on the array, Alexa Fluor 488–labeled goat anti-human IgM (catalog no. A-21249, Thermo Fisher Scientific; diluted at 1:400) in TSM binding buffer was used for detection. Heatmap and correlation map of binding preferences were analyzed using GLAD (Glycan Array Dashboard; www.glycotoolkit.com/Tools/GLAD/).

CFG glycan microarray

The CFG glycan microarray version 5.0 was used (www.functionalglycomics.org) (*78*). Briefly, purified anti-Tn antibodies (C1; diluted to 10 μg/ml) in TSM binding buffer were added to the array slides for 1 hour at RT. Alexa Fluor 488–labeled goat anti-human IgM at 1:400 dilution in TSM binding buffer was used for detection. Slides were analyzed as described in the "Tn glycopeptide microarray" section.

Generation and characterization of *Cosmc*KO Dakiki cells using CRISPR-Cas9 system

Generation of CosmcKO cells

Human B cell line (Dakiki) was purchased from American Type Culture Collection (ATCC; TIB-206) and cultured in RPMI 1640 medium (Corning) supplemented with 20% (v/v) FBS and penicillin-streptomycin (200 U/ml; Thermo Fisher Scientific) at 37°C and 5% CO_2. The single-guide RNA sequence (Dharmacon) to target *Cosmc* gene is described in fig. S4. Dakiki cells were infected by spinoculation. Tn positivity serves as a cell surface marker of *Cosmc*KO. Cells were first selected using drug and then sorted for Tn-positive population using ReBaGs6 on a cell sorter (MoFlo Astrios EQ Sorter, Beckman Coulter). The resultant homogenous cell population was termed *Cosmc*KO cells.

Characterization of CosmcKO cells

First, we analyzed whole-cell extracts from WT and *Cosmc*KO Dakiki cells that were resolved on SDS-PAGE and immunoblotted for Cosmc, T-synthase, and β-actin using anti-Cosmc antibody (catalog no. sc-271829, H-10, Santa Cruz Biotechnology), anti-T-synthase antibody (catalog no. sc-100745, F-31, Santa Cruz Biotechnology), or anti-β-actin antibody (catalog no. sc-47778, C4, Santa Cruz Biotechnology) at 1:1000 dilution in TBST with 1% nonfat milk. Secondary detection was performed with HRP-labeled goat anti-mouse IgG (H+L) antibody (catalog no. 115-035-003, Jackson ImmunoResearch Laboratories Inc.) at 1:10,000 dilution in TBST containing 0.5% nonfat milk. For lectin blots, cell extracts (~30 μg) were pretreated with 50 mU of neuraminidase in 50 mM sodium acetate (pH 5.0) for 1 hour at 37°C following the manufacturer's instructions and analyzed by SDS-PAGE-lectin blots. Biotinylated peanut agglutinin (catalog no. B-1075-5, Vector Laboratories; diluted to 1 μg/ml) or HPA (catalog no. L6512, Sigma-Aldrich; diluted to 1 μg/ml) in TBST containing 1% BSA was used as the primary reagent. Secondary detection was performed with HRP-labeled streptavidin at 1:10,000 dilution in TBST containing 0.5% BSA.

For the Tn expression levels on the cell surface in *Cosmc*KO Dakiki cell line, cells were incubated with 100 μl of a murine anti-Tn antibody (ReBaGs6; diluted to 1 μg/ml) or mouse isotype IgM (diluted to 1 μg/ml) in PBS for 1 hour on ice. Cells were washed twice with 3 ml of cold PBS by centrifugation and incubated with 100 μl of Alexa Fluor 488–labeled goat anti-mouse IgM antibody at 1:400 dilution in PBS for 1 hour on ice in the dark. After washing twice with 3 ml of cold PBS by centrifugation, cells were resuspended in 500 μl of PBS and then analyzed on a flow cytometer (FACSCalibur, Becton Dickinson).

The T-synthase enzyme activity was fluorescently assayed using 4-methylumbelliferyl 2-acetamido-2-deoxy-α-D-galactopyranoside (catalog no. EM04782, Biosynth Carbosynth) as an acceptor substrate and uridine 5′-diphosphate–galactose (MU06699, Biosynth Carbosynth) as donor sugar as described previously (*79*). For a control, α-mannosidase activity was assayed using 4-methylumbelliferyl α-D-mannopyranoside (catalog no. M3657, Sigma-Aldrich) as an acceptor substrate. The T-synthase activity was normalized as a ratio of T-synthase activity:α-mannosidase activity in Dakiki WT cells. The purification procedure of IgA1 from Dakiki cell lines was previously described (*35*).

Tn(+)IgA1 binding study by purified anti-Tn antibodies

*Cosmc*KO Dakiki cells were established as described above. Purification of IgA1 from Dakiki cell line was previously described (*35*). Purified IgA1 with or without extended *O*-glycans was analyzed by SDS-PAGE WB as described in the "Affinity purification of putative anti-Tn antibodies and WB" section with some modifications. WB was performed using our purified anti-Tn antibodies (10 μg/ml) in TBST containing 0.5% BSA as the primary antibody. VVA lectin blotting was performed as described above.

Microbead flow cytometry: Diagnostic assay

Asialo-BSM (100 mg) and HPA (1 mg; catalog no. L3382, Sigma-Aldrich) were conjugated to 5×10^6 Polybead carboxylate 6.0-μm microspheres (2×10^7 beads/ml; catalog no. 17141, Polysciences Inc.) following the manufacturer's instructions. For detection of anti-Tn IgM in sera, ~5×10^4 Asialo-BSM microbeads were incubated with 100 μl of serum (diluted at 1:100 in PBS) for 1 hour on ice. For controls, ~5×10^4 Asialo-BSM microbeads were incubated with isotype human IgM (3.3 μg/ml) or serial diluted Asialo-BSM–purified anti-Tn IgM (starting at 3.3 μg/ml) from human sera (catalog no. 7323901, Lampire Biological Laboratories Inc., PA) for 1 hour on ice. The beads were washed twice with 1 ml of chilled 1 M NaCl (beads pelleted 850*g* for 30 s) and incubated with 100 μl of Alexa Fluor 488–labeled goat anti-human IgM (μ chain) antibody at 1:400 dilution in PBS for 1 hour on ice in the dark. For detection of Tn(+)IgA1 in sera, ~5×10^4 HPA microbeads were incubated with 100 μl of serum (diluted at 1:100 in PBS) for 1 hour on ice. For controls, 5×10^4 HPA microbeads were incubated with purified Tn(+)IgA1 or Tn(−)IgA1 (10 μg/ml) from Dakiki cell lines for 1 hour on ice. The beads were washed twice with 1 ml of cold PBS and incubated with 100 μl of FITC-labeled mouse anti-human IgA1 antibody at 1:400 dilution in PBS for 1 hour on ice in the dark. After washing the beads twice with 1 ml of cold PBS, the beads were resuspended in 500 μl of chilled PBS and analyzed on a flow cytometer (FACSCalibur, Becton Dickinson). Total serum IgM in sera was measured by an ELISA kit (catalog no. 88-50620-22, Thermo Fisher Scientific). Total serum IgA in sera was measured by an ELISA kit (catalog no. 88-50600-22, Thermo Fisher Scientific).

Preparation of BN-APAGE

CICs were resolved using BN-APAGE system as previously described (*34*). Samples and unstained native markers (catalog no. LC0725, Invitrogen) were mixed with the sample buffer [0.5% Coomassie blue G-250 and 50 mM ε-aminocaproic acid in 10 mM bis-tris (pH 7.5) at final concentration] just before use, and electrophoresis was performed using 1× anode buffer [50 mM bis-tris HCl (pH 7.0)] and 1× cathode buffer [50 mM tricine, 15 mM bis-tris, and 0.0015% G-250 (pH 7.0)] for at ~18 hours using relatively low voltage and low current (e.g., 15 to 20 V, ~2 mA, for four gels).

WB on BN-APAGE

Protein samples (~0.1 μg) or plain serum (1:200 dilution in PBS, 10 μl loaded) run on BN-APAGE was transferred onto activated polyvinylidene difluoride membrane (catalog no. IPVH00010, EMD Millipore, wet-transfer system; 40 V for 2 hours). The membranes were quickly destained with 100% methanol, washed with TBST, and blocked with 5% (w/v) nonfat milk in TBST for 1 hour at RT. The blocked membranes were incubated with HRP-labeled goat anti-human IgM (μ chain) antibody or goat anti-mouse IgM (μ chain) antibody (catalog no. 115-035-020, Jackson ImmunoResearch Laboratories Inc.) at 1:10,000 dilution in TBST containing 1% nonfat milk for 1 hour at RT, and the signals were detected onto the autoradiography films (catalog no. 1141 J52, HyBlot CL, Thomas Scientific) using SuperSignal West Pico Chemiluminescent Substrate.

Immunodepletion experiment

Approximately 10 μl (50% slurry in PBS) of goat anti-human IgA (α chain) agarose beads (catalog no. A2691, Sigma-Aldrich) or isotype goat IgG control beads (catalog no. ab104155, Abcam) were added to the equal amount of purified anti-Tn CICs (~0.1 μg). After 2 hours of incubation in cold room (10 rpm), unbound/depleted fractions were collected after centrifugation at 850*g* for 30 s and analyzed by WB using the BN-APAGE system.

Glycomimetic treatment of anti-Tn CICs and BN-APAGE analysis

For glycomimetic treatment, purified anti-Tn CICs (~0.1 μg) were pretreated with α-methylGalNAc (100 mM), α-methylGlcNAc (100 mM), or mock in PBS for 2 hours at 4°C on a rotator (10 rpm), and the samples were analyzed by BN-APAGE WB and probed for IgM and IgA.

ELISA-based glycomimetic inhibition assays

IgA1 glycopeptides (0.01 μg per well; ID 18 or ID 19 as listed in Table 2) were immobilized using immobilization buffer ($NaHCO_3$/Na_2CO_3, pH 9.6) in a 96-well plate (Thermo Fisher Scientific, PolySorp) overnight at 4°C. The plate was washed three times with TSM containing 0.05% Tween 20 (TSMT) and added 5% (w/v) BSA in TSMT for 1 hour at RT. The plate was incubated with purified anti-Tn CICs (1 μg/ml) from IgAN serum [P3 and pooled P1 to P10 (Pmix)] or healthy donors [C3 and pooled C1 to C10 (Cmix)] in TSMT containing 0.5% BSA for 1 hour at RT. The plate was washed three times with TSMT and incubated for 1 hour with HRP-conjugated goat anti-human IgM at 1:1000 dilution in TSMT containing 0.5% BSA at RT. The plate was washed three times with TSMT and developed using 3,3',5,5'-Tetramethylbenzidine substrate solution (catalog no. ab171523, Abcam) for 30 min, and the reaction was stopped with 1 N HCl. Absorbance (450 nm) was read on an ImageXpress Pico (Molecular Devices). The IC_{50} was calculated with GraphPad Prism 6.0 (GraphPad Software Inc.) after subtraction from ID 19 as a baseline. For inhibition assay, purified anti-Tn CICs were preincubated with a serial dilution (1:3) of α-methylGalNAc or DiαGalNAc (starting at 10 mM) for 30 min at RT.

Immunofluorescence on human primary mesangial cells

HRMCs (catalog no. 4200, ScienCell) were cultured, as described in the protocol of the company, on poly-L-lysine–coated (2 μg/cm^2; catalog no. 0403) cover strip in 24-well plate. Cells were harvested at ~90% confluency and fixed with 4% paraformaldehyde (PFA) (catalog no. 50-980-487, Thermo Fisher Scientific) with 0.05% Triton X-100 in PBS for 20 min at 4°C. Fixed cells were blocked with 5% (v/v) goat serum (catalog no. 16210064, Thermo Fisher Scientific) in PBS for 1 hour at 4°C and incubated with anti-Tn CICs (1 μg/ml) and anti-vimentin antibody (catalog no. sc-6260, V9, mouse IgG, Santa Cruz Biotechnology; diluted to 1:400) in PBS overnight at 4°C. Cells were washed three times with chilled PBS and incubated with Alexa Fluor 488–labeled goat anti-human IgM and Alexa Fluor 633–labeled goat anti-mouse IgG (catalog no. A21052, Thermo Fisher Scientific) at 1:400 dilution in PBS for 1 hour at 4°C in the dark.

Cells were washed three times with chilled PBS and stained with 4′,6-diamidino-2-phenylindole (DAPI) (catalog no. 9542, Sigma-Aldrich; diluted to 0.1 μM) in PBS for 10 min at RT and analyzed by confocal microscope (Zeiss Axioimager Z1; ×630 magnification). Anti-Tn CICs from three healthy controls (C3, C6, and Cmix) and three IgAN (P5, P10, and Pmix) were used on this assay. For isotype control, human IgM, IgG, and IgA (1 μg/ml each) or mouse IgG (catalog no. 0107-01, SouthernBiotech; diluted to 0.5 μg/ml) in PBS was used. All images were taken in three different areas in 24-well plate.

Cell surface staining by anti-Tn CICs

HRMCs (~5×10^5) were stained with anti-Tn CICs (5 μg/ml) purified from IgAN (P5, P10, or Pmix) or healthy control (C3, C6, or Cmix) for 1 hour at 4°C. After washing three times with 2 ml of cold PBS, cells were incubated with Alexa Fluor 488–labeled goat anti-human IgM (μ chain), goat anti-human IgG (H+L), or FITC-labeled mouse anti-human IgA1 at 1:400 dilution in PBS for 1 hour on ice. After washing three times with 2 ml of cold PBS, cells were resuspended in 500 μl of chilled PBS and analyzed on a flow cytometer (FACSCalibur, Becton Dickinson). Mean fluorescent intensity (MFI) (FL1-H) for each staining was plotted on a graph.

Cell proliferation assay

Serum (~500 μl) was mixed with 50 μl of Tn(+)matrix beads or mock beads overnight at 4°C (10 rpm). Supernatant was collected after pelleting the beads at 500*g* for 30 s at 4°C. After two rounds of such sequential anti-Tn CIC immunodepletion (serum-ID) and its control (serum-mock), collected serum was filtered by syringe filter unit (catalog no. SLHP033RS, MilliporeSigma) before use. Cells were cultured at ~90% confluency in 96-well plate and starved in mesangial cell medium (catalog no. 4201) with 0.5% FBS (catalog no. 0010) and 0.05× mesangial cell growth supplement (catalog no. 4252) from ScienCell for 24 hours at 37°C before stimulation. Cells were stimulated with 5% serum-mock and 5% serum-ID with or without exogenous anti-Tn CICs (total, 50 ng/100 μl per well) for 24 hours at 37°C incubator. Cells were fixed with 4% PFA with 0.05% Triton X-100 in PBS for 20 min at 4°C. Fixed cells were blocked with 5% (v/v) goat serum in PBS for 1 hour at 4°C and incubated with anti–Ki-67 antibody (SP6, rabbit IgG, catalog no. CRM325B, Biocare Medical; diluted to 1:50) in PBS for 1 hour at 4°C. Cells were washed three times with chilled PBS and incubated with Alexa Fluor 488–labeled goat anti-rabbit IgG (catalog no. A27034, Thermo Fisher Scientific) at 1:400 dilution in PBS for 1 hour at 4°C in the dark. Cells were washed three times with chilled PBS, stained with DAPI (diluted to 0.1 μM) in PBS for 10 min at RT, and analyzed using a microscope (AMG EVOS FL digital inverted microscope, Thermo Fisher Scientific; ×400 magnification). For inhibition assay, anti-Tn CICs were preincubated with 100 mM α-methylGalNAc or α-methylGlcNAc in PBS for 30 min at RT. Serum from three healthy controls (C3, C6, and Cmix) and three IgAN (P5, P10, and Pmix) was used in this assay. For cell proliferation studies using plain serum from patients with IgAN and healthy controls, HRMCs were starved as described above, and cells were stimulated with 1, 2.5, or 5% serum with IgAN (Pmix) or healthy control (Cmix) for 24 hours in a 37°C cell culture incubator. For the comparison of cell proliferation studies, cells were stimulated with 2.5% serum with IgAN (P1 to P20) or healthy control (C1 to C20) for 24 hours at 37°C incubation. One microliters of serum with IgAN (P1 to P20) or healthy control (C1 to C20) was analyzed on SDS-PAGE gel and stained with Coomassie.

For control cell staining, HEK293T cells (catalog no. CRL-3216, ATCC) were starved in Dulbecco's modified Eagle's medium (catalog no. 10-013-CV, Corning) with 0.5% FBS for 24 hours at 37°C before stimulation. Cells were stimulated with 5% serum with IgAN (mock), CIC-immunodepleted serum (ID), or exogenously adding CICs from IgAN (ID + anti-Tn CICs) for 24 hours at 37°C CO_2 incubator. Serum and anti-Tn CICs (P10 or Pmix) were used in this assay. In parallel, healthy control serum and HRMCs were also used as described above. All images were taken in three different areas in 96-well plate, and Ki-67–positive cells were counted. All images were taken in three different areas in 96-well plate, and Ki-67–positive cells were counted.

WB analysis for complement C3 using purified anti-Tn CICs

Purified anti-Tn CICs (~0.1 μg) from three healthy controls (C3, C6, and Cmix) and three patients with IgAN (P5, P10, and Pmix) were analyzed on SDS-PAGE as described. Membranes were blocked with 5% milk in TBST for 1 hour at RT and incubated with a recombinant anti-C3 antibody (EPR2988, catalog no. ab181147, rabbit IgG, Abcam; diluted at 1:1000 in TBST) for 1 hour at RT. HRP-labeled goat anti-rabbit IgG (catalog no. 5220-0336, KPL) at 1:10,000 dilution was used for detection. The signals were detected using SuperSignal West Pico Chemiluminescent Substrate on an Amersham Imager 600.

Protein identification by MS

Proteins (~5 μg) were resolved using SDS-PAGE shown in fig. S2, and the appropriate bands were excised and processed for in-gel trypsin treatment as described elsewhere (*80*). The next day, the supernatant was removed from the gel pieces, and 50 μl of 50% acetonitrile was added and incubated on the shaker for 10 min at RT. Both supernatants were combined and dried in a SpeedVac concentrator. The samples were taken up in 15 μl of water and diluted two times in 0.1% formic acid.

Each sample (2 μl) was used for C18 reversed-phase liquid chromatography–MS using an Ultimate 3000 nanoLC coupled to an Orbitrap Fusion Lumos mass spectrometer (both Thermo Fisher Scientific). Samples were loaded onto a C18 precolumn (C18 PepMap 100, 300 μm by 5 mm, 5 μm, 100 Å, Thermo Fisher Scientific) with solvent A at 15 μl/min [0.1% formic acid (FA) in H_2O] for 3 min and separated on a C18 analytical column (picofrit 75-μm inside diameter by 150 mm, 3 μm, New Objective) using a linear gradient of 2 to 45% solvent B (80% acetonitrile and 0.1% FA) over 39 min at 400 nl/min. The mass spectrometer was operated under following conditions: The ion source parameters have a spray voltage of 2100 V and ion transfer tube temperature of 200°C. MS scans were performed in the Orbitrap at a resolution of 60,000 within a scan range of mass/charge ratio (m/z) 400 to 1600, a radio frequency (RF) lens of 30%, and Automatic Gain Control (AGC) target of 1×10^5 for a maximum injection time of 50 ms. The top 15 precursors were selected for MS/MS (MS^2) in a data-dependent manner, within a mass range of m/z 400 to 1600 and a minimum intensity threshold of 1×10^5 and an isolation width of 2 m/z. Higher-energy C-trap dissociation (HCD) was performed in stepped collision energy mode of 30% (±5%) and detected in the Orbitrap with a resolution of 30,000 with the first mass at m/z 120, an AGC target of 2×10^5, and a maximum injection of 250 ms.

Data analysis was performed against the human SWISS-PROT database (version 2016-05-11) using SEQUEST through proteome discoverer (version 2.1.0.81, Thermo Fisher Scientific) under the

following settings: trypsin (two missed cleavage sites), precursor mass tolerance of 10 parts per million, and fragment mass tolerance of 0.02 Da. Dynamic modifications were oxidation on Met, deamidation on Asn, phosphorylation on Ser/Thr, and N-terminal acetylation. Static modifications were carbamidomethyl on Cys. False discovery rate was set to 1%. Main protein hits were sorted on the basis of their number of peptide spectrum matches (PSMs). The identified peptides are listed in table S1.

Synthesis of DiαGalNAc and DiαGlcNAc

The synthesis began with the α-linked glycosidation of chloroethyl linker to *N*-acetylgalactosamine (**1**) by using AcCl at 70°C (fig. S17). Thioacetyl substitution to **2** was successful using potassium thioacetate (KSAc) in *N*,*N*′-dimethylformamide (DMF), which gave **3** in high yield. To dimerize this substrate, the thioacetyl group was removed to expose the thiol using sodium methoxide in methanol, and compound **2** was introduced to perform a direct S_N2 displacement of the halide to render **4** in 33% yield (DiαGalNAc). The synthesis of the DiαGlcNAc was repeated in a similar fashion as described above to render **8** from *N*-acetylglucosamine (**5**) with comparable yields (fig. S17).

General considerations

All commercially available reagents and solvents were used without further purification. All reactions described were conducted under argon atmosphere in an oven-dried glassware. ^{1}H nuclear magnetic resonance (NMR), ^{13}C NMR, and two-dimensional NMR experiments were performed on a Varian MR 400-MHz spectrometer. The spectral data were reported relative to deuterated peaks [dimethyl sulfoxide (DMSO)–d_6, δ2.50], and chemical shifts were reported in parts per million (δ). ^{1}H NMR splitting patterns were designated as singlet (s), doublet (d), triplet (t), doublet of doublets (dd), apparent triplet (app. t.), or multiplet (m), and coupling constants were reported in hertz. Thin-layer chromatography (TLC) was developed on glass-backed TLC plates (silica gel 60 with a 254-nm fluorescent indicator and 250-mm layer thickness) that were stored over drierite in a desiccator. TLC plates were visualized by coating with ammonium molybdate/cerium(IV) sulfate stain heated mildly on a hot plate. Flash column chromatography was performed on silica gel (32 to 63 μm) with reported solvent systems in v/v ratios. Reversed-phase high-performance liquid chromatography (RP-HPLC) was performed using Waters (Method A) Gradient Purification System 2767 equipped with Waters 2489 ultraviolet/visible detection module and Waters 2545 Binary Gradient Module using a C18 100A (250 mm by 30 mm; Phenomenex) column (PREPARATORY). Ultraflex II matrix–assisted laser desorption ionization time-of-flight MS (MALDI-TOF MS) was used to analyze samples cocrystallized using super 2,5-Dihydroxybenzoic acid (DHB) matrix.

2-Chloroethyl 2-acetamido-2-deoxy-α-D-galactopyranoside (**2**): Compound **2** was made according to a previous protocol (*81*). 2-Acetylthio 2-acetamido-2-deoxy-α-D-galactopyranoside (**3**): Potassium thioacetate [3.0 equivalent (equiv.)] was slowly added to a solution containing compound 2 (1.0 equiv.) in DMF and stirred for 16 hours at RT. Upon completion, water was added to quench the reaction and concentrated in vacuo. Flash column chromatography using $CHCl_3$ and MeOH system (10:1, v/v) gave compound **3** in 84% yield as a brown solid [radiofrequency field (R_f) = 0.1]. ^{1}H NMR (400 MHz, DMSO-d_6): δ 7.50 ppm (d, J = 8.4 Hz, 1H), 4.69 ppm (d, J = 3.6 Hz, 1H), 4.53 to 4.56 ppm (m, 2H), 4.43 ppm (br, 1H), 3.99 to 4.05 ppm (m, 1H), 3.72 ppm (br, 1H), 3.56 to 3.63 ppm (m, 3H), 3.43 to 3.54 ppm (m, 3H), (td, J = 1.6, 6.2 Hz, 2H), 2.33 ppm (s, 3H), and 1.84 ppm (s, 3H). ^{13}C NMR (125 MHz, DMSO-d_6): δ 195.09 ppm, 169.65 ppm, 97.44 ppm, 71.53 ppm, 68.04 ppm, 67.39 ppm, 65.86 ppm, 60.60 ppm, 49.73 ppm, 30.54 ppm, 28.38 ppm, and 22.69 ppm.

α-D-2-Ethylthio 2-acetamido-galactopyranosyl α-D-2-Ethylthio 2-acetamido-galactopyranoside (**4**): Compound **3** dissolved in methanol was added NaOMe (1.2. equiv.), and the reaction was stirred for 30 min at RT. Compound **2** (1.1 equiv.) predissolved in MeOH was added to the reaction mixture and refluxed for 2.5 hours. Reaction was quenched using acetic acid and concentrated in vacuo. Purification using RP-HPLC gave compound **4** in 33% yield as a white lyophilizate. [RP-HPLC condition: solvent A, water + 0.1% trifluoroacetic acid (TFA); solvent B, acetonitrile. 0 to 5 min, 2% B; 5 to 16 min, 10% B; 16 to 19 min, 15% B; 19 to 23 min, 100% B; 23 to 25 min, 2% B. 4, retention time (R_t) = 8.26 min]. ^{1}H NMR (400 MHz, DMSO-d_6): δ 7.46 to 7.55 ppt (m, 2H), 4.74 ppt (dd, J = 2.8, 16.4 Hz, 2H), 4.43 to 4.56 ppt (m, 2H), 3.96 to 4.08 ppt (m, 4H), 3.44 to 3.77 ppt (m, 10H), 2.67 to 2.72 ppt (m, 4H), and 1.84 ppt (s, 3H). ^{13}C NMR (125 MHz, DMSO-d_6): δ 169.62 ppt, 97.62 ppt, 71.51 ppt, 68.12 ppt, 67.71 ppt, 67.40 ppt, 49.67 ppt, 43.63 ppt, 31.00 ppt, and 22.68 ppt. MALDI-TOF analysis of 4: calculated [M + H$^+$] ($C_{20}H_{36}N_2NaO_{12}S^+$) = 551.1 *m*/*z*; observed [M + H$^+$] ($C_{20}H_{36}N_2NaO_{12}S^+$) = 551.0 *m*/*z*.

2-Chloroethyl 2-acetamido-2-deoxy-α-D-glucopyranoside (**6**): Compound 6 was made according to a previous protocol (*81*). α-D-2-Ethylthio 2-acetamido-glucopyranosyl α-D-2-ethylthio 2-acetamido-glucopyranoside (**8**): Potassium thioacetate (3.0 equiv.) was slowly added to a solution containing compound 6 (1.0 equiv.) in DMF and stirred for 16 hours at RT. Upon completion, water was added to quench the reaction and concentrated in vacuo. NaOMe (1.2. equiv.) was added to the crude containing compound **7** dissolved in methanol, and the reaction was stirred for 30 min at RT. Compound **6** (1.1 equiv.) predissolved in MeOH was added to the reaction mixture and refluxed for 2.5 hours. Reaction was quenched using acetic acid and concentrated in vacuo. Purification using RP-HPLC gave compound **8** in 30% yield as a white lyophilizate. (RP-HPLC condition: solvent A, water + 0.1% TFA; solvent B, acetonitrile. 0 to 5 min, 2% B; 5 to 16 min, 10% B; 16 to 19 min, 15% B; 19 to 23 min, 100% B; 23 to 25 min, 2% B. 8, R_t = 8.53 min).^{1}H NMR (400 MHz, DMSO-d_6): δ 7.60 to 7.65 (m, 2H), 4.71 to 4.77 (m, 2H), 4.61 (d, J = 11.2, 1H), 4.47 to 4.52 (m, 1H), 3.42 to 3.81 (m, 12H), 3.11 to 3.21 (m, 2H), 2.67 to 2.76 (m, 4H), and 1.84 (s, 3H). ^{13}C NMR (125 MHz, DMSO-d_6): δ 169.58, 96.88, 72.95, 70.79, 70.63, 67.07, 60.85, 53.79, 31.02, and 22.62. MALDI-TOF analysis of 8: calculated [M + H$^+$] ($C_{20}H_{36}N_2NaO_{12}S^+$) = 551.1 *m*/*z*; observed [M + H$^+$] ($C_{20}H_{36}N_2NaO_{12}S^+$) = 551.0 *m*/*z*.

Statistical analysis

Data were analyzed using Student's *t* test (two-tailed), and the differences were considered statistically significant at $P < 0.05$.

SUPPLEMENTARY MATERIALS

Supplementary material for this article is available at https://science.org/doi/10.1126/sciadv.abm8783

REFERENCES AND NOTES

1. J. Berger, N. Hinglais, Intercapillary deposits of IgA-IgG. *J. Urol. Nephrol. (Paris)* **74**, 694–695 (1968).
2. R. J. Wyatt, B. A. Julian, IgA nephropathy. *N. Engl. J. Med.* **368**, 2402–2414 (2013).

3. S. Jarrick, S. Lundberg, A. Welander, J.-J. Carrero, J. Höijer, M. Bottai, J. F. Ludvigsson, Mortality in IgA nephropathy: A nationwide population-based cohort study. *J. Am. Soc. Nephrol.* **30**, 866–876 (2019).
4. T. Knoop, B. E. Vikse, E. Svarstad, S. Leh, A. V. Reisæter, R. Bjørneklett, Mortality in patients with IgA nephropathy. *Am. J. Kidney Dis.* **62**, 883–890 (2013).
5. C. C. Geddes, V. Rauta, C. Gronhagen-Riska, L. P. Bartosik, A. G. Jardine, L. S. Ibels, Y. Pei, D. C. Cattran, A tricontinental view of IgA nephropathy. *Nephrol. Dial. Transplant.* **18**, 1541–1548 (2003).
6. E. Imai, K. Yamagata, K. Iseki, H. Iso, M. Horio, H. Mkino, A. Hishida, S. Matsuo, Kidney disease screening program in Japan: History, outcome, and perspectives. *Clin. J. Am. Soc. Nephrol.* **2**, 1360–1366 (2007).
7. B.-S. Cho, W.-H. Hahn, H. I. Cheong, I. Lim, C. W. Ko, S.-Y. Kim, D.-Y. Lee, T.-S. Ha, J.-S. Suh, A nationwide study of mass urine screening tests on Korean school children and implications for chronic kidney disease management. *Clin. Exp. Nephrol.* **17**, 205–210 (2013).
8. H. Suzuki, K. Kiryluk, J. Novak, Z. Moldoveanu, A. B. Herr, M. B. Renfrow, R. J. Wyatt, F. Scolari, J. Mestecky, A. G. Gharavi, B. A. Julian, The pathophysiology of IgA nephropathy. *J. Am. Soc. Nephrol.* **22**, 1795–1803 (2011).
9. B. Knoppova, C. Reily, N. Maillard, D. V. Rizk, Z. Moldoveanu, J. Mestecky, M. Raska, M. B. Renfrow, B. A. Julian, J. Novak, The origin and activities of IgA1-containing immune complexes in IgA nephropathy. *Front. Immunol.* **7**, 117 (2016).
10. I. Beerman, J. Novak, R. J. Wyatt, B. A. Julian, A. G. Gharavi, The genetics of IgA nephropathy. *Nat. Clin. Pract. Nephrol.* **3**, 325–338 (2007).
11. A. Toraño, Y. Tsuzukida, Y. S. Liu, F. W. Putnam, Location and structural significance of the oligosaccharides in human Ig-A1 and IgA2 immunoglobulins. *Proc. Natl. Acad. Sci. U.S.A.* **74**, 2301–2305 (1977).
12. Y. Ohyama, M. B. Renfrow, J. Novak, K. Takahashi, Aberrantly glycosylated IgA1 in IgA nephropathy: What we know and what we don't know. *J. Clin. Med.* **10**, 3467 (2021).
13. E. Tarelli, A. C. Smith, B. M. Hendry, S. J. Challacombe, S. Pouria, Human serum IgA1 is substituted with up to six O-glycans as shown by matrix assisted laser desorption ionisation time-of-flight mass spectrometry. *Carbohydr. Res.* **339**, 2329–2335 (2004).
14. K. Takahashi, S. B. Wall, H. Suzuki, A. D. Smith IV, S. Hall, K. Poulsen, M. Kilian, J. A. Mobley, B. A. Julian, J. Mestecky, J. Novak, M. B. Renfrow, Clustered *O*-glycans of IgA1: Defining macro- and microheterogeneity by use of electron capture/transfer dissociation. *Mol. Cell. Proteomics* **9**, 2545–2557 (2010).
15. J. Mestecky, M. Tomana, Z. Moldoveanu, B. A. Julian, H. Suzuki, K. Matousovic, M. B. Renfrow, L. Novak, R. J. Wyatt, J. Novak, Role of aberrant glycosylation of IgA1 molecules in the pathogenesis of IgA nephropathy. *Kidney Blood Press. Res.* **31**, 29–37 (2008).
16. A. C. Allen, S. J. Harper, J. Feehally, Galactosylation of N- and O-linked carbohydrate moieties of IgA1 and IgG in IgA nephropathy. *Clin. Exp. Immunol.* **100**, 470–474 (1995).
17. S. Lehoux, R. Mi, R. P. Aryal, Y. Wang, K. T.-B. G. Schjoldager, H. Clausen, I. van Die, Y. Han, A. B. Chapman, R. D. Cummings, T. Ju, Identification of distinct glycoforms of IgA1 in plasma from patients with immunoglobulin A (IgA) nephropathy and healthy individuals. *Mol. Cell. Proteomics* **13**, 3097–3113 (2014).
18. R. C. Monteiro, L. Halbwachs-Mecarelli, M. C. Roque-Barreira, L. H. Noel, J. Berger, P. Lesavre, Charge and size of mesangial IgA in IgA nephropathy. *Kidney Int.* **28**, 666–671 (1985).
19. K. N. Lai, J. C. K. Leung, L. Y. Y. Chan, M. A. Saleem, P. W. Mathieson, F. M. Lai, S. C. W. Tang, Activation of podocytes by mesangial-derived TNF-α: Glomerulo-podocytic communication in IgA nephropathy. *Am. J. Physiol. Renal Physiol.* **294**, F945–F955 (2008).
20. M. A. DeCicco RePass, N. Bhat, J. Heimburg-Molinaro, S. Bunnell, R. D. Cummings, H. D. Ward, Molecular cloning, expression, and characterization of UDP N-acetyl-α-D-galactosamine: Polypeptide N-acetylgalactosaminyltransferase 4 from *Cryptosporidium parvum*. *Mol. Biochem. Parasitol.* **221**, 56–65 (2018).
21. J. Heimburg-Molinaro, J. W. Priest, D. Live, G.-J. Boons, X. Song, R. D. Cummings, J. R. Mead, Microarray analysis of the human antibody response to synthetic Cryptosporidium glycopeptides. *Int. J. Parasitol.* **43**, 901–907 (2013).
22. G. F. Springer, H. Tegtmeyer, Origin of anti-Thomsen-Friedenreich (T) and Tn agglutinins in man and in White Leghorn chicks. *Br. J. Haematol.* **47**, 453–460 (1981).
23. G. F. Springer, R. E. Horton, Blood group isoantibody stimulation in man by feeding blood group-active bacteria. *J. Clin. Invest.* **48**, 1280–1291 (1969).
24. J. Mestecky, J. Novak, Z. Moldoveanu, M. Raska, IgA nephropathy enigma. *Clin. Immunol.* **172**, 72–77 (2016).
25. M. Tomana, K. Matousovic, B. A. Julian, J. Radl, K. Konecny, J. Mestecky, Galactose-deficient IgA1 in sera of IgA nephropathy patients is present in complexes with IgG. *Kidney Int.* **52**, 509–516 (1997).
26. M. Tomana, J. Novak, B. A. Julian, K. Matousovic, K. Konecny, J. Mestecky, Circulating immune complexes in IgA nephropathy consist of IgA1 with galactose-deficient hinge region and antiglycan antibodies. *J. Clin. Invest.* **104**, 73–81 (1999).
27. F. P. Schena, A. Pastore, N. Ludovico, R. A. Sinico, S. Benuzzi, V. Montinaro, Increased serum levels of IgA1-IgG immune complexes and anti-F(ab')2 antibodies in patients with primary IgA nephropathy. *Clin. Exp. Immunol.* **77**, 15–20 (1989).
28. T. Yanagihara, R. Brown, S. Hall, Z. Moldoveanu, A. Goepfert, M. Tomana, B. A. Julian, J. Mestecky, J. Novak, *In vitro*-generated immune complexes containing galactose-deficient IgA1 stimulate proliferation of mesangial cells. *Results Immunol.* **2**, 166–172 (2012).
29. J. A. Tumlin, M. P. Madaio, R. Hennigar, Idiopathic IgA nephropathy: Pathogenesis, histopathology, and therapeutic options. *Clin. J. Am. Soc. Nephrol.* **2**, 1054–1061 (2007).
30. T. Ju, R. D. Cummings, A unique molecular chaperone Cosmc required for activity of the mammalian core 1 beta 3-galactosyltransferase. *Proc. Natl. Acad. Sci. U.S.A.* **99**, 16613–16618 (2002).
31. Y. Wang, T. Ju, X. Ding, B. Xia, W. Wang, L. Xia, M. He, R. D. Cummings, Cosmc is an essential chaperone for correct protein O-glycosylation. *Proc. Natl. Acad. Sci. U.S.A.* **107**, 9228–9233 (2010).
32. R. P. Aryal, T. Ju, R. D. Cummings, The endoplasmic reticulum chaperone Cosmc directly promotes in vitro folding of T-synthase. *J. Biol. Chem.* **285**, 2456–2462 (2010).
33. T. Ju, Y. Wang, R. P. Aryal, S. D. Lehoux, X. Ding, M. R. Kudelka, C. Cutler, J. Zeng, J. Wang, X. Sun, J. Heimburg-Molinaro, D. F. Smith, R. D. Cummings, Tn and sialyl-Tn antigens, aberrant *O*-glycomics as human disease markers. *Proteomics Clin. Appl.* **7**, 618–631 (2013).
34. R. P. Aryal, P. B. Kwak, A. G. Tamayo, M. Gebert, P.-L. Chiu, T. Walz, C. J. Weitz, Macromolecular assemblies of the mammalian circadian clock. *Mol. Cell* **67**, 770–782.e6 (2017).
35. Y. Matsumoto, M. R. Kudelka, M. S. Hanes, S. Lehoux, S. Dutta, M. B. Jones, K. A. Stackhouse, G. E. Cervoni, J. Heimburg-Molinaro, D. F. Smith, T. Ju, E. L. Chaikof, R. D. Cummings, Identification of Tn antigen O-GalNAc-expressing glycoproteins in human carcinomas using novel anti-Tn recombinant antibodies. *Glycobiology* **30**, 282–300 (2020).
36. J. Novak, M. Tomana, R. Brown, S. Hall, L. Novak, B. A. Julian, R. J. Wyatt, J. Mestecky, K. Matousovic, IgA1-containing immune complexes in IgA nephropathy differentially affect proliferation of mesangial cells. *Kidney Int.* **67**, 504–513 (2005).
37. I. C. Moura, M. Arcos-Fajardo, C. Sadaka, V. Leroy, M. Benhamou, J. Novak, F. Vrtovsnik, E. Haddad, K. R. Chintalacharuvu, R. C. Monteiro, Glycosylation and size of IgA1 are essential for interaction with mesangial transferrin receptor in IgA nephropathy. *J. Am. Soc. Nephrol.* **15**, 622–634 (2004).
38. K. Y. Tam, J. C. K. Leung, L. Y. Y. Chan, M. F. Lam, S. C. W. Tang, K. N. Lai, Macromolecular IgA1 taken from patients with familial IgA nephropathy or their asymptomatic relatives have higher reactivity to mesangial cells in vitro. *Kidney Int.* **75**, 1330–1339 (2009).
39. C. Czerkinsky, W. J. Koopman, S. Jackson, J. E. Collins, S. S. Crago, R. E. Schrohenloher, B. A. Julian, J. H. Galla, J. Mestecky, Circulating immune complexes and immunoglobulin A rheumatoid factor in patients with mesangial immunoglobulin A nephropathies. *J. Clin. Invest.* **77**, 1931–1938 (1986).
40. D. V. Rizk, N. Maillard, B. A. Julian, B. Knoppova, T. J. Green, J. Novak, R. J. Wyatt, The emerging role of complement proteins as a target for therapy of IgA nephropathy. *Front. Immunol.* **10**, 504 (2019).
41. N. Maillard, R. J. Wyatt, B. A. Julian, K. Kiryluk, A. Gharavi, V. Fremeaux-Bacchi, J. Novak, Current understanding of the role of complement in IgA nephropathy. *J. Am. Soc. Nephrol.* **26**, 1503–1512 (2015).
42. J. C. Jennette, The immunohistology of IgA nephropathy. *Am. J. Kidney Dis.* **12**, 348–352 (1988).
43. A. J. Woodroffe, A. A. Gormly, P. E. McKenzie, A. M. Wootton, A. J. Thompson, A. E. Seymour, A. R. Clarkson, Immunologic studies in IgA nephropathy. *Kidney Int.* **18**, 366–374 (1980).
44. T. M. Eison, M. C. Hastings, Z. Moldoveanu, J. T. Sanders, L. Gaber, P. D. Walker, K. K. Lau, B. A. Julian, J. Novak, R. J. Wyatt, Association of IgG co-deposition with serum levels of galactose-deficient IgA1 in pediatric IgA nephropathy. *Clin. Nephrol.* **78**, 465–469 (2012).
45. R. Katafuchi, H. Nagae, K. Masutani, K. Tsuruya, K. Mitsuiki, Comprehensive evaluation of the significance of immunofluorescent findings on clinicopathological features in IgA nephropathy. *Clin. Exp. Nephrol.* **23**, 169–181 (2019).
46. C. Heybeli, M. A. Oktan, S. Yıldız, H. Ü. Arda, M. Ünlü, C. Çavdar, A. Sifil, A. Çelik, S. Sarıoğlu, T. Çamsarı, Clinical significance of mesangial IgM deposition in patients with IgA nephropathy. *Clin. Exp. Nephrol.* **23**, 371–379 (2019).
47. S. S. Bellur, S. Troyanov, H. T. Cook, I. S. D. Roberts; Working Group of the International IgA Nephropathy Network and the Renal Pathology Society, Immunostaining findings in IgA nephropathy: Correlation with histology and clinical outcome in the Oxford classification patient cohort. *Nephrol. Dial. Transplant.* **26**, 2533–2536 (2011).
48. I. S. D. Roberts, Pathology of IgA nephropathy. *Nat. Rev. Nephrol.* **10**, 445–454 (2014).
49. Y. Wada, H. Ogata, Y. Takeshige, A. Takeshima, N. Yoshida, M. Yamamoto, H. Ito, E. Kinugasa, Clinical significance of IgG deposition in the glomerular mesangial area in patients with IgA nephropathy. *Clin. Exp. Nephrol.* **17**, 73–82 (2013).
50. P. M. Zeis, E. Kavazarakis, L. Nakopoulou, M. Moustaki, A. Messaritaki, M. P. Zeis, P. Nicolaidou, Glomerulopathy with mesangial IgM deposits: Long-term follow up of 64 children. *Pediatr. Int.* **43**, 287–292 (2001).

51. Z. Moldoveanu, H. Suzuki, C. Reily, K. Satake, L. Novak, N. Xu, Z. Q. Huang, B. Knoppova, A. Khan, S. Hall, H. Yanagawa, R. Brown, C. J. Winstead, D. B. O'Quinn, A. Weinmann, A. G. Gharavi, K. Kiryluk, B. A. Julian, C. T. Weaver, Y. Suzuki, J. Novak, Experimental evidence of pathogenic role of IgG autoantibodies in IgA nephropathy. *J. Autoimmun.* **118**, 102593 (2021).
52. D. V. Rizk, M. K. Saha, S. Hall, L. Novak, R. Brown, Z. Q. Huang, H. Fatima, B. A. Julian, J. Novak, Glomerular immunodeposits of patients with IgA nephropathy are enriched for IgG autoantibodies specific for galactose-deficient IgA1. *J. Am. Soc. Nephrol.* **30**, 2017–2026 (2019).
53. R. B. Cejas, V. Lorenz, Y. C. Garay, F. J. Irazoqui, Biosynthesis of O-N-acetylgalactosamine glycans in the human cell nucleus. *J. Biol. Chem.* **294**, 2997–3011 (2019).
54. K. Giannakakis, S. Feriozzi, M. Perez, T. Faraggiana, A. O. Muda, Aberrantly glycosylated IgA1 in glomerular immune deposits of IgA nephropathy. *J. Am. Soc. Nephrol.* **18**, 3139–3146 (2007).
55. Y. D. Neugut, K. Kiryluk, Genetic determinants of IgA nephropathy: Western perspective. *Semin. Nephrol.* **38**, 443–454 (2018).
56. T. Ju, K. Brewer, A. D'Souza, R. D. Cummings, W. M. Canfield, Cloning and expression of human core 1 β1,3-galactosyltransferase. *J. Biol. Chem.* **277**, 178–186 (2002).
57. K. Kiryluk, Y. Li, Z. Moldoveanu, H. Suzuki, C. Reily, P. Hou, J. Xie, N. Mladkova, S. Prakash, C. Fischman, S. Shapiro, R. A. LeDesma, D. Bradbury, I. Ionita-Laza, F. Eitner, T. Rauen, N. Maillard, F. Berthoux, J. Floege, N. Chen, H. Zhang, F. Scolari, R. J. Wyatt, B. A. Julian, A. G. Gharavi, J. Novak, GWAS for serum galactose-deficient IgA1 implicates critical genes of the *O*-glycosylation pathway. *PLOS Genet.* **13**, e1006609 (2017).
58. S. Hu, H. Bao, X. Xu, X. Zhou, W. Qin, C. Zeng, Z. Liu, Increased miR-374b promotes cell proliferation and the production of aberrant glycosylated IgA1 in B cells of IgA nephropathy. *FEBS Lett.* **589**, 4019–4025 (2015).
59. K. Yamada, N. Kobayashi, T. Ikeda, Y. Suzuki, T. Tsuge, S. Horikoshi, S. N. Emancipator, Y. Tomino, Down-regulation of core 1 β1,3-galactosyltransferase and Cosmc by Th2 cytokine alters *O*-glycosylation of IgA1. *Nephrol. Dial. Transplant.* **25**, 3890–3897 (2010).
60. W. Qin, Q. Zhou, L.-C. Yang, Z. Li, B.-H. Su, H. Luo, J.-M. Fan, Peripheral B lymphocyte β1,3-galactosyltransferase and chaperone expression in immunoglobulin A nephropathy. *J. Intern. Med.* **258**, 467–477 (2005).
61. Q. Sun, J. Zhang, N. Zhou, X. Liu, Y. Shen, DNA methylation in Cosmc promoter region and aberrantly glycosylated IgA1 associated with pediatric IgA nephropathy. *PLOS ONE* **10**, e0112305 (2015).
62. D. P. Gale, K. Molyneux, D. Wimbury, P. Higgins, A. P. Levine, B. Caplin, A. Ferlin, P. Yin, C. P. Nelson, H. Stanescu, N. J. Samani, R. Kleta, X. Yu, J. Barratt, Galactosylation of IgA1 is associated with common variation in *C1GALT1*. *J. Am. Soc. Nephrol.* **28**, 2158–2166 (2017).
63. F. Malycha, T. Eggermann, M. Hristov, F. P. Schena, P. R. Mertens, K. Zerres, J. Floege, F. Eitner, No evidence for a role of cosmc-chaperone mutations in European IgA nephropathy patients. *Nephrol. Dial. Transplant.* **24**, 321–324 (2008).
64. K. S. Buck, A. C. Smith, K. Molyneux, H. el-Barbary, J. Feehally, J. Barratt, B-cell *O*-galactosyltransferase activity, and expression of *O*-glycosylation genes in bone marrow in IgA nephropathy. *Kidney Int.* **73**, 1128–1136 (2008).
65. R. Coppo, B. Basolo, G. Martina, C. Rollino, M. de Marchi, F. Giacchino, G. Mazzucco, M. Messina, G. Piccoli, Circulating immune complexes containing IgA, IgG and IgM in patients with primary IgA nephropathy and with Henoch-Schoenlein nephritis. Correlation with clinical and histologic signs of activity. *Clin. Nephrol.* **18**, 230–239 (1982).
66. K. Suzuki, K. Honda, K. Tanabe, H. Toma, H. Nihei, Y. Yamaguchi, Incidence of latent mesangial IgA deposition in renal allograft donors in Japan. *Kidney Int.* **63**, 2286–2294 (2003).
67. R. Sinniah, Occurrence of mesangial IgA and IgM deposits in a control necropsy population. *J. Clin. Pathol.* **36**, 276–279 (1983).
68. B. Ernst, J. L. Magnani, From carbohydrate leads to glycomimetic drugs. *Nat. Rev. Drug Discov.* **8**, 661–677 (2009).
69. M. Mannik, Mechanisms of tissue deposition of immune complexes. *J. Rheumatol. Suppl.* **14** (Suppl. 13), 35–42 (1987).
70. M. Mannik, Pathophysiology of circulating immune complexes. *Arthritis Rheum.* **25**, 783–787 (1982).
71. S. Brasil, C. Pascoal, R. Francisco, D. Marques-da-Silva, G. Andreotti, P. A. Videira, E. Morava, J. Jaeken, V. D. R. Ferreira, CDG therapies: From bench to bedside. *Int. J. Mol. Sci.* **19**, 1304 (2018).
72. J. H. Park, J. Reunert, M. He, R. G. Mealer, M. Noel, Y. Wada, M. Grüneberg, J. Horváth, R. D. Cummings, O. Schwartz, T. Marquardt, L-Fucose treatment of FUT8-CDG. *Mol. Genet Metab. Rep.* **25**, 100680 (2020).
73. T. Marquardt, K. Lühn, G. Srikrishna, H. H. Freeze, E. Harms, D. Vestweber, Correction of leukocyte adhesion deficiency type II with oral fucose. *Blood* **94**, 3976–3985 (1999).
74. D. Cagdas, M. Yılmaz, N. Kandemir, İ. Tezcan, A. Etzioni, Ö. Sanal, A novel mutation in leukocyte adhesion deficiency type II/CDGIIc. *J. Clin. Immunol.* **34**, 1009–1014 (2014).
75. H. K. Harms, K. P. Zimmer, K. Kurnik, R. M. Bertele-Harms, S. Weidinger, K. Reiter, Oral mannose therapy persistently corrects the severe clinical symptoms and biochemical abnormalities of phosphomannose isomerase deficiency. *Acta Paediatr.* **91**, 1065–1072 (2002).
76. C. J. Hendriksz, P. McClean, M. J. Henderson, D. G. Keir, V. C. Worthington, F. Imtiaz, E. Schollen, G. Matthijs, B. G. Winchester, Successful treatment of carbohydrate deficient glycoprotein syndrome type 1b with oral mannose. *Arch. Dis. Child.* **85**, 339–340 (2001).
77. A. Borgert, J. Heimburg-Molinaro, X. Song, Y. Lasanajak, T. Ju, M. Liu, P. Thompson, G. Ragupathi, G. Barany, D. F. Smith, R. D. Cummings, D. Live, Deciphering structural elements of mucin glycoprotein recognition. *ACS Chem. Biol.* **7**, 1031–1039 (2012).
78. J. Heimburg-Molinaro, X. Song, D. F. Smith, R. D. Cummings, Preparation and analysis of glycan microarrays. *Curr. Protoc. Protein Sci.* **Chapter 12**, Unit 12.10 (2011).
79. T. Ju, R. D. Cummings, A fluorescence-based assay for Core 1 β3galactosyltransferase (T-synthase) activity. *Methods Mol. Biol.* **1022**, 15–28 (2013).
80. R. Plomp, P. J. Hensbergen, Y. Rombouts, G. Zauner, I. Dragan, C. A. M. Koeleman, A. M. Deelder, M. Wuhrer, Site-specific N-glycosylation analysis of human immunoglobulin e. *J. Proteome Res.* **13**, 536–546 (2014).
81. Q. Wang, S. A. Ekanayaka, J. Wu, J. Zhang, Z. Guo, Synthetic and immunological studies of 5'-*N*-phenylacetyl sTn to develop carbohydrate-based cancer vaccines and to explore the impacts of linkage between carbohydrate antigens and carrier proteins. *Bioconjug. Chem.* **19**, 2060–2067 (2008).

Acknowledgments: We thank T. R. McKitrick, A. M. McQuillan, and R. Barnes for help with data collection and analysis of the array; A. Y. Mehta for printing glycopeptide/glycan array; and C. Gao in the NCFG at BIDMC for assistance with GLAD toolkit. We thank S. Cummings for helpful discussions and timely resource management for the project. We thank J. Zeng and the other members of the Cummings laboratory for helpful discussions. **Funding:** This work was supported by the National Institute of Health, grants R01DK080876, P41GM103694, and R24GM137763 (to R.D.C.). **Author contributions:** R.D.C. conceived the project. Y.M. and R.P.A. designed and executed most of the experiments except diagnostic assay, which was performed by Y.M. R.P.A., Y.M., and R.D.C. wrote the manuscript. J.H.-M. supervised all glycopeptide and CFG array data and analysis and reviewed and edited the manuscript. K.S. generated and analyzed MS data. S.L. generated *Cosmc*KO Dakiki cells. S.S.P., W.J.W., and E.L.C. were responsible for generating and characterizing synthetic version of dimeric glycomimetic compounds. J.A.E.v.W., I.V.D., and A.B.C. provided clinical IgAN serum samples. All authors reviewed and approved the manuscript for submission. R.D.C. provided funding. **Competing interests:** The authors declare that they have no competing interests. **Data and materials availability:** All data needed to evaluate the conclusions in the paper are present in the paper and/or Supplementary Materials with no restrictions. The DiαGalNAc can be provided by E.L.C. pending scientific review and a completed material transfer agreement. Requests for the DiαGalNAc should be submitted to echaikof@bidmc.harvard.edu.

Submitted 19 October 2021
Accepted 12 September 2022
Published 28 October 2022
10.1126/sciadv.abm8783